

國立交通大學

統計學研究所

碩士論文

監控隨機效應線型品質特性之製程

Monitoring Linear Profiles based on a Random-effect Model



中華民國九十五年六月

# 監控隨機效應線型品質特性之製程

## Monitoring Linear Profiles based on a Random-effect Model

研 究 生：陳瑩琪  
指 導 教 授：洪志真

Student : Ying-Chi Chen  
Advisor : Dr. Jyh-Jen Horng Shiau

國 立 交 通 大 學

統計學研究所

碩 士 論 文

A Thesis

Submitted to Institute of Statistics  
College of Science  
National Chiao Tung University  
in Partial Fulfillment of the Requirements  
for the Degree of  
Master  
in  
Statistics  
June 2006  
Hsinchu, Taiwan, Republic of China

中華民國九十五年六月

# 監控隨機效應線型品質特性之製程

研究生： 陳瑩琪

指導教授： 洪志真 博士

國立交通大學統計學研究所

## 摘要

監控製程與產品之剖面(profile)資料在統計品質管制中是一個非常熱門且有前景的研究領域。我們的研究將以對具有隨機效應之線型資料(linear profile)的監控方法為主，目的在使模型能容許更多合理的變異來處理實際的問題。我們發現，若我們忽略應該被納入模型的變異，而用固定效應的模型來做製程監控，則假警報的比率會非常高。

對隨機效應的資料模型，我們用三個 Shewhart-type 管制圖分別對線型資料的三個參數作監控。在製程監控之第二階段中，因為三個監控統計量是相互獨立的，我們分配同樣的假警報比率給三個統計量，從而控制整個製程的假警報率為事先設計的比率  $\alpha$ 。

在製程監控之第一階段中，不同資料所對應的監控統計量並不獨立，但是對任一條線型資料而言，三個監控統計量是相互獨立的。因此，在第一個階段中，我們分別用 Bonferroni 方法和 Multiple FDR 方法來控制整個歷史資料的假警報率(overall false-alarm rate)，並且比較這兩種方法的優劣。模擬的結果顯示，若以偵測力為判斷方法優劣的標準，用 Multiple FDR 方法較 Bonferroni 方法好，特別是當歷史資料中超出管制界限的線型資料愈多時。用 Multiple FDR 方法使偵測力增加的代價是將歷史資料中在管制狀態下的線型資料誤判為失控狀態的比率會略為提高。

# Monitoring Linear Profiles based on a Random-effect Model

Student : Ying-Chi Chen    Advisor : Dr. Jyh-Jen Horng Shiau

Institute of Statistic  
National Chiao Tung University

## ABSTRACT

The monitoring of process and product profiles is a very popular and promising area of research in statistical process control. This study proposes a monitoring scheme for linear profiles with a random-effect model to incorporate the subject-to-subject variation in some real-life problems. It is found that if we ignore the subject-to-subject variation and monitor the process by the existing scheme based on the fixed-effect model, the false-alarm rate could be incredibly high.

For random-effect models, we use three Shewhart-type control charts to monitor linear profiles. In Phase II operation, since the three monitoring statistics are mutually independent, we give the same in-control false-alarm rate to each control chart such that the overall in-control false alarm rate of the combined-chart scheme is controlled at the prescribed level  $\alpha$ .

In Phase I operation, the monitoring statistics across profiles are not independent, but the three monitoring statistics for the same profile are mutually independent. Therefore, to control the overall false-alarm rate in Phase I monitoring, the Bonferroni method and Multiple FDR method are implemented and compared. Simulation results show that the Multiple FDR method is better than the Bonferroni method in terms of detecting power, especially when more out-of-control profiles are in the historical data. The tradeoff of using the Multiple FDR method is the slightly larger “false-alarm rate”, which is defined as the proportion of the false alarms within the in-control profiles in the historical data.

## 誌 謝

在統研所短短的兩年裡，我得到了很多，除了書本上的知識，也交到了很多好朋友。這篇論文的完成，最要感謝我的指導老師 洪志真教授認真親切的指導跟辛勤的批閱，還有博士班碩慧學姊，無論是在學業上或生活上的指教及協助，使我能夠順利地完成論文。最後還要感謝我的研究所同學冠達、清峰、明曄、火哥跟勢耀帶給我充滿歡笑的回憶，在學業上的切磋討論也使我獲益甚多。

此外還要感謝家人給我的體諒與支持，使我可以無後顧之憂的專心學習，最後僅將此論文獻給我最愛的家人、朋友們。



陳 瑩 琪      謹誌于  
國立交通大學統計研究所  
中華民國九十五年六月

# Contents

<b>1. INTRODUCTION .....</b>	<b>1</b>
<b>2. LITERATURE REVIEW.....</b>	<b>4</b>
<b>3. MODEL AND METHODS.....</b>	<b>11</b>
3.1. Model Assumptions.....	11
3.2. SPC with a Random-effect Model.....	11
3.3. Monitoring Statistics and their Distributions.....	13
3.4. Phase II method.....	16
3.5. Phase I method .....	18
3.5.1. <i>Bonferroni method</i> .....	19
3.5.2. <i>Multiple FDR method</i> .....	20
<b>4. SIMULATION RESULTS.....</b>	<b>22</b>
4.1. Phase II.....	22
4.1.1. <i>Settings</i> .....	22
4.1.2. <i>Three Shewhart-type Control Charts</i> .....	23
4.1.3. <i>When the Fixed-effect Model is Mistakenly Used</i> .....	24
4.2. Phase I .....	27
<b>5. CONCLUSION .....</b>	<b>29</b>

<b>6. APPENDIX.....</b>	<b>31</b>
Proof of Property 1. ....	31
Proof of Property 2. ....	31
Proof of Property 3. ....	32
Proof of Property 4. ....	32
<b>7. REFERENCES.....</b>	<b>33</b>
<b>TABLES .....</b>	<b>35</b>
<b>FIGURES .....</b>	<b>48</b>



# 1. Introduction

Control charts, as a primary tool in statistical process control (SPC), have been successfully applied in a variety of industries since Shewhart introduced the technique in 1924. DeVor, Chang, and Sutherland (1992) and Montgomery (2005) reviewed various kinds of control charts and monitoring schemes. For traditional control chart applications, it is assumed that the quality of a process or product can be suitably represented by the distribution of a univariate quality characteristic or by the multivariate distribution of a vector consisting of several quality characteristics. However, in many practical situations, the quality of a process or a product is better characterized by a relationship between a response variable and one or more explanatory variables. Instead of observing a single measurement on each sampled product item, we obtain a set of measurements, which when plotted takes the shape of a curve or a surface. These curve data are referred to as profiles in the literature. Kang and Albin (2000) gave an example of a product characterized by a profile, in which the response variable is the amount of aspartame (an artificial sweetener) that can be dissolved per liter of water and the explanatory variable is temperature. Shiau and Weng (2004) proposed a nonlinear curve profile monitoring scheme by nonparametric regression.

In particular, there have been interests in monitoring processes which are characterized by linear profiles in recent years. Most of the studies related to monitoring such linear profiles have been motivated by calibration applications. Kang and Albin (2000) gave an example that arises in semiconductor manufacturing. They proposed a method to monitor the MFC, the mass flow controller, which controls the flow of gases in semiconductor manufacturing. If



an MFC is in control, then the measured pressure (P) in the chamber is approximately a linear function of the set point for flow (X). Kim et al. (2003) studied the same problem as that in Kang and Albin (2000) but proposed an alternative method for linear profile monitoring. Another example presented in Mahmoud and Woodall (2004) aims at studying the stability of the calibration curve in the photometric determination of  $\text{Fe}^{3+}$  with sulfosalicylic acid. In this example, the relationship between the response variable (the absorbance of the solution) and the explanatory variable (the concentration of the solution) is a linear function. Mahmoud, Woodall, Reynolds, Vining, Birch, and Smith (2004) proposed a method based on using indicator variables in Phase I analysis.

The above authors treated the intercept and the slope term of the linear profiles under study as fixed but unknown parameters. They modeled the profiles by a simple linear regression model:

$$y_{ij} = A_0 + A_1 x_i + \varepsilon_{ij}, \quad i = 1, \dots, n, \quad j = 1, 2, \dots,$$

where the response  $y_{ij}$  is the  $i^{\text{th}}$  observation of the  $j^{\text{th}}$  profile measured at the  $i^{\text{th}}$  sampled point,  $x_i$  is the  $i^{\text{th}}$  set point, intercept  $A_0$  and slope  $A_1$  are constants to be estimated. This is a model commonly used in calibration profile monitoring.

However, under this model, the batch effect, the change of humidity or temperature, the characteristics of the measuring equipment, and other hard-to-control factors that may affect the response variable, are all categorized as part of the random error  $\varepsilon_{ij}$ . This simplified model may not be appropriate for many applications in which these factors vary over time and may affect the values of the intercept and slope of the linear profile. By their nature, these

hard-to-control factors should be considered as common causes of variations. A monitoring scheme constructed based on the above “fixed-effect” model may interpret these common-cause variations as special-cause variations and signal many false alarms. Thus, we need a model that can cope with these common-cause variations and construct a monitoring scheme accordingly.

With this perspective,  $A_0$  and  $A_1$  in the above linear regression model are no longer fixed parameters for such applications; instead, they are random variables with legitimate variations represented by distributions. Thus, we adopt a random-effect model  $y_{ij} = A_{0j} + A_{1j}x_i + \varepsilon_{ij}$ , where  $A_{0j}$  and  $A_{1j}$  are random variables. With this random-effect model, we incorporate more variability into the response variable in order to reduce false alarms, and thus avoid over adjustments.

For monitoring the incoming profiles in Phase II operation, we consider three Shewhart-type control charts to monitor intercept, slope, and error variance respectively in this thesis. We remark that the EWMA version of these charts can be extended easily. To control the overall in-control false-alarm rate  $\alpha$  for the combined-chart scheme, through the independence property of the three charts, we control the same individual in-control false-alarm rate at level  $1 - (1 - \alpha)^{1/3}$  for each of the three charts.

In Phase I operation, one of the goals is to detect and remove out-of-control profiles in the historical dataset. Note that the monitoring statistics across the historical profiles are not independent. Thus, we use the Bonferroni method to control the familywise error rate (FWER), which is referred to as the overall false-alarm rate in SPC context. As it is well known, the Bonferroni method can be quite conservative sometimes, which may cause a dramatic loss in detecting

power. To meet our goal in Phase I and to enhance the detecting power, we also consider controlling the false discovery rate (FDR) proposed by Benjamini and Hochberg (1995) instead of controlling the FWER. In this thesis, we extend the procedure provided in Benjamini and Hochberg (1995) to deal with multiple charts in Phase I profile monitoring and call it the Multiple FDR method.

The rest of thesis is organized as follows. Section 2 reviews the Phase II operation proposed by Kim et al. (2003) and describes the Phase I operation by controlling FDR. Section 3 introduces our random-effect model and proposes the monitoring schemes for Phase II and Phase I respectively. Section 4 presents results of the simulation studies. It is found that the Multiple FDR method indeed is better than the Bonferroni method in terms of the “true-alarm rate”, the rate of detecting real out-of-control profiles in Phase I operation. Section 5 concludes the thesis with a brief summary and some remarks.



## 2. Literature Review

For Phase II operation, Kang and Albin (2000) considered representing linear profiles by the model

$$y_{ij} = A_0 + A_1 x_i + \varepsilon_{ij}, i=1,2,\dots,n, j=1,2,\dots, \quad (1)$$

where the intercept term  $A_0$  and the slope term  $A_1$  are fixed parameters, and the  $\varepsilon_{ij}$ 's are independent and identically distributed (i.i.d.) normal random variables with mean zero and variance  $\sigma_e^2$ . In their method, for the  $j^{\text{th}}$  profile, the estimators of  $A_0$  and  $A_1$ , denoted by  $a_{0j}$  and  $a_{1j}$  respectively, are given by the following formulas:

$$a_{0j} = \bar{y}_j - a_{1j}\bar{x} \quad \text{and} \quad a_{1j} = \frac{S_{xy(j)}}{S_{xx}},$$

where  $\bar{y}_j = \frac{1}{n} \sum_{i=1}^n y_{ij}$ ,  $\bar{x} = \frac{1}{n} \sum_{i=1}^n x_i$ ,  $S_{xy(j)} = \sum_{i=1}^n (x_i - \bar{x})y_{ij}$ , and  $S_{xx} = \sum_{i=1}^n (x_i - \bar{x})^2$ .

Since  $a_{0j}$  and  $a_{1j}$  are not independent, they used a bivariate  $T^2$  chart to monitor  $A_0$  and  $A_1$  simultaneously in Phase II operation.

To improve Kang and Albin's method, Kim et al. (2003) proposed an alternative approach. First, they coded the X-values by centering so that the average of the coded values is zero. This results in the independence of the estimators of intercept and slope and eliminates much of the need for the  $T^2$  approach. After coding the X-values, they obtained an alternative form of the model as  $y_{ij} = B_0 + B_1 x_i^* + \varepsilon_{ij}$ ,  $i=1,2,\dots,n$ , where  $B_0 = A_0 + A_1 \bar{x}$ ,  $B_1 = A_1$ , and  $x_i^* = x_i - \bar{x}$ . For the  $j^{\text{th}}$  profile, the estimators of  $B_0$  and  $B_1$ , denoted by  $b_{0j}$  and  $b_{1j}$  respectively, are given by the following formulas:

$$b_{0j} = \bar{y}_j \quad \text{and} \quad b_{1j} = \frac{S_{xy(j)}}{S_{xx}},$$

where  $\bar{y}_j = \frac{1}{n} \sum_{i=1}^n y_{ij}$ ,  $S_{xy(j)} = \sum_{i=1}^n x_i^* y_{ij}$  and  $S_{xx} = \sum_{i=1}^n x_i^{*2}$ .

Since  $b_{0j}$  and  $b_{1j}$  are independent, Kim et al. (2003) constructed separate control charts to monitor  $b_{0j}$  and  $b_{1j}$ . Also, they used the values of  $\text{MSE}_j$  (i.e., the usual estimator of  $\sigma_e^2$  based on the residuals corresponding to the fitted line of sample  $j$ ) to monitor  $\sigma_e^2$ , the variance of the error term  $\varepsilon_{ij}$ . It is well known that  $\hat{\sigma}_e^2$  is independent of  $b_{0j}$  and  $b_{1j}$  by the linear regression theory. Therefore, they used three separate EWMA charts to monitor respectively the intercept, the slope, and the variance of the error term in Phase

II operation.

The three EWMA charts proposed by Kim et al. (2003) are used jointly, in the sense that out-of-control signals can come from any of the three charts. The basic motivation for their approach comes from the fact that when assignable causes are present in a process for which the output of a product is characterized by a linear profile, at least one of the three parameters, intercept, slope, or error variance, will be affected. Also, having a control chart corresponding to each parameter leads to easier diagnoses of out-of-control signals compared with the  $T^2$  chart given in Kang and Albin (2000).

In Kim et al.'s method, for monitoring the intercept  $B_0$ , they used the estimates  $b_{0j}$  of the intercept to compute the EWMA statistics

$$EWMA_I(j) = \theta b_{0j} + (1 - \theta)EWMA_I(j-1), j=1,2,\dots,$$

with  $\theta$  ( $0 < \theta \leq 1$ ) being a smoothing constant and the initial value  $EWMA_I(0)$  is the in-control value of  $B_0$ . An out-of-control signal is given as soon as

$EWMA_I(j) < LCL$  or  $EWMA_I(j) > UCL$ , where

$$LCL = B_0 - L_I \sigma \sqrt{\frac{\theta}{(2 - \theta)n}} \quad \text{and} \quad UCL = B_0 + L_I \sigma \sqrt{\frac{\theta}{(2 - \theta)n}},$$

with  $L_I(>0)$  chosen to give a specified in-control average run length (ARL).

The estimates  $b_{1j}$  of the slope  $B_1$  are used in the EWMA chart for monitoring the slope. The EWMA statistics are given by

$$EWMA_S(j) = \theta b_{1j} + (1 - \theta)EWMA_S(j-1), j=1,2,\dots,$$

with  $\theta$  ( $0 < \theta \leq 1$ ) being a smoothing constant and  $EWMA_S(0)$  is the

in-control value of  $B_1$ . The control limits for the chart are given by

$$LCL = B_1 - L_s \sigma \sqrt{\frac{\theta}{(2-\theta)S_{xx}}} \quad \text{and} \quad UCL = B_1 + L_s \sigma \sqrt{\frac{\theta}{(2-\theta)S_{xx}}},$$

where  $L_s(>0)$  is chosen to give a specified in-control ARL.

For the EWMA chart of monitoring the error variance ( $\sigma_e^2$ ), they used the value of  $MSE_j$  to obtain the EWMA statistics. Unlike the two EWMA charts mentioned above, this chart is a one-sided EWMA chart to detect only increases in process variability. The EWMA statistics are given by

$$EWMA_E(j) = \max\{\theta \ln(MSE_j) + (1-\theta)EWMA_E(j-1), \ln(\sigma_0^2)\}, j=1,2,\dots,$$

with  $\theta$  ( $0 < \theta \leq 1$ ) being a smoothing constant and  $EWMA_E(0) = \ln(\sigma_0^2)$ , where  $\sigma_0^2$  is the in-control value of  $\sigma_e^2$ . The control limit for the chart is given by

$$UCL = L_E \sqrt{\frac{\theta}{(2-\theta)} \text{Var}[\ln(MSE_j)]},$$

where  $L_E(>0)$  is chosen to give a specified in-control ARL.

Kim et al. (2003) claimed that their method is better than Kang and Albin's in terms of the ARLs. In other words, for intercept shifts, slope shifts, or increases in error variance, Kim et al.'s method can detect shifts faster than Kang and Albin's in Phase II operation.

Later, we will adopt Kim et al.'s approach to develop our Phase II method based on a random-effect model. However, we will use three univariate Shewhart-type control charts instead of three univariate EWMA charts in Phase II operation.

For Phase I operation, by control charting, we actually are performing a statistical test to each of the profiles in the historical dataset to determine if it is in control. This resembles the multiple-test problem in hypothesis testing. If each profile is monitored with a conventional individual in-control false-alarm rate, say, 0.0027, then the overall in-control false-alarm rate of our monitoring scheme may be inflated to an undesirable level, especially when the number of profiles in the dataset is large. The common approach to the multiple-test problem is to control the FWER, which is similar to the overall false-alarm rate in our context. Benjamini and Hochberg (1995) gave an argument about controlling the FWER as follows. Classical procedures that control the FWER at a level conventional for single-comparison problems tend to have substantially less power than the per comparison procedure of the same level. Luckily, often the control of the FWER is not quite needed. The control of the FWER is important when a conclusion from the various individual inferences could be wrong (e.g., committing a type I error) when at least one of them is wrong. This may be the case, for example, when several new treatments are competing against a standard one, and a single treatment is chosen from the set of treatments which are declared significantly better than the standard one.

On the other hand, a treatment group and a control group are often compared by testing various aspects of the effects. The overall conclusion that the treatment is superior needs not be wrong even if some of the null hypotheses are falsely rejected. Therefore, Benjamini and Hochberg (1995) proposed a new approach to the multiple-test problem. It calls for controlling the expected proportion of falsely rejected hypotheses called the false discovery rate, FDR. They considered the problem of testing simultaneously  $k$

hypotheses, among which  $k_0$  are true. Let  $R$  be the number of hypotheses being rejected. Table 1 summarizes the situations in a traditional form. The specific  $k$  hypotheses are assumed to be known in advance.  $R$  is an observable random variable, while  $k_0 - R_0$ ,  $R_0$ ,  $k_1 - R_1$ ,  $R_1$  are unobservable random variables. They used the lower-case letters to stand for their realized values.

Benjamini and Hochberg (1995) suggested that the proportion of the errors committed by falsely rejecting null hypotheses can be viewed through the random variable  $Q = R_0/(R_0 + R_1)$ . They defined  $Q=0$  when  $R_0 + R_1 = 0$ , as no error of false rejection can be made in such case. Note that  $Q$  is unobservable, as we know neither  $R_0$  nor  $R_1$ . So,  $q = r_0/(r_0 + r_1)$  is unknown even after experimentation. Hence, they defined the false discovery rate  $Q_e$  to be the expectation of  $Q$ . That is,

$$Q_e = E(Q) = E\left(\frac{R_0}{R_0 + R_1}\right) = E\left(\frac{R_0}{R}\right).$$

Benjamini and Hochberg (1995) also showed two important properties of the FDR. First, if all null hypotheses are true, the FDR is equal to the FWER. Second, when  $k_0 < k$ , the FDR is smaller than or equal to the FWER. Therefore, any procedure that controls the FWER also controls the FDR. On the other hand, if the procedure controls the FDR only, it can be less stringent and hence gain more power than a procedure controlling the FWER, and the gain in power gets larger when more of the hypotheses are non-true.

Benjamini and Hochberg (1995) provided a simple procedure to control the FDR at a prescribed level  $q^*$ . The procedure is described as follows.



Consider testing  $H_1, H_2, \dots, H_k$  based on the corresponding p-values  $P_1, P_2, \dots, P_k$ . Let  $P_{(1)} \leq P_{(2)} \leq \dots \leq P_{(k)}$  be the ordered p-values and  $H_{(j)}$  be the null hypothesis with the p-value corresponding to  $P_{(j)}$ . Let  $l$  be the largest  $j$  for which  $P_{(j)} \leq \frac{j}{k} q^*$ . If such  $l$  exists, reject all  $H_{(j)}$ ,  $j=1, 2, \dots, l$ ; otherwise, no hypotheses are rejected.

Benjamini and Hochberg (1995) had shown that for independent test statistics and for any configuration of false null hypotheses, the above procedure controls the FDR at level  $q^*$ . They concluded that the power of the FDR-controlling method is uniformly larger than that of the FWER-controlling method. Also, the advantage increases with the number of the non-true null hypotheses. Finally, the advantage increases in  $k$ . Therefore, the loss of power as  $k$  increases is relatively small for the FDR-controlling method compared with the FWER-controlling method. Furthermore, the independence of the test statistics is not needed for the above assertions to hold.

In our SPC context, if the goal is simply to decide if all the historical data are stable or not, then controlling the FWER is the criterion to suit the purpose. However, if the goal is to select in-control profiles, it can still be met even some in-control profiles are falsely rejected. In this sense, for the purpose of Phase I operation, it seems that we do not need a criterion as stringent as controlling the FWER and controlling the FDR may be a reasonable alternative. Later, we will develop our Phase I method by controlling the FDR to improve the power of detecting out-of-control profiles from the historical linear profile data. To cope with the issue of using three charts to monitor the intercept, slope, and error variance separately, we extend the original FDR method to a Multiple

FDR method and conduct a comparison study between the Bonferroni method and Multiple FDR method by simulation. We find that, as expected, improvements are gained by the Multiple FDR method.

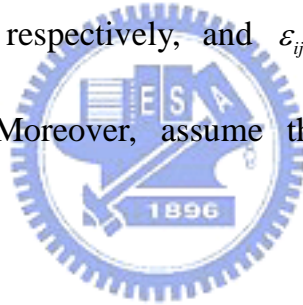
### 3. Model and Methods

#### 3.1. Model Assumptions

Assume a linear random-effect model for the linear profiles:

$$y_{ij} = A_{0j} + A_{1j}x_i + \varepsilon_{ij}, i=1, \dots, n, j=1, 2, \dots, \quad (2)$$

where  $A_{0j}$ 's and  $A_{1j}$ 's are independent and identically distributed as  $N(\alpha_0, \sigma_0^2)$  and  $N(\alpha_1, \sigma_1^2)$ , respectively, and  $\varepsilon_{ij}$ 's are i.i.d. random errors distributed as  $N(0, \sigma_e^2)$ . Moreover, assume that  $A_{0j}$ ,  $A_{1j}$ , and  $\varepsilon_{ij}$  are mutually independent.



#### 3.2. SPC with a Random-effect Model

How do we judge whether the process is out of control when the process data is represented by a linear random-effect model? Since  $A_{0j} \sim N(\alpha_0, \sigma_0^2)$  and  $A_{1j} \sim N(\alpha_1, \sigma_1^2)$ ,  $\alpha_0$  and  $\alpha_1$  represent some characteristics of  $A_{0j}$  and  $A_{1j}$ , respectively. If the estimate  $\hat{\alpha}_0$  or  $\hat{\alpha}_1$  of a linear profile does not fall within a certain range, we suspect that the distribution of  $A_{0j}$  or  $A_{1j}$  has changed (i.e., the mean of  $A_{0j}$  or  $A_{1j}$  has shifted). Hence, we propose monitoring the process by monitoring the mean  $\alpha_0$  of the intercept term  $A_{0j}$  and  $\alpha_1$  of the

slope term  $A_{1j}$ . Also, as in the fixed-effect model, we can monitor the variance of the error term,  $\sigma_e^2$ , as well. To sum up, we propose to monitor the process by using the estimators  $\hat{\alpha}_0$ ,  $\hat{\alpha}_1$ , and  $\hat{\sigma}_e^2$ . To construct control limits for these monitoring statistics, we need to have their distributions. Details are given in Subsection 3.3.

In control-chart implementation for SPC applications, it usually consists of two stages, Phase I and Phase II. A major goal of Phase I is to collect a set of in-control data to establish an in-control baseline for Phase II to construct appropriate control limits for on-line process monitoring. Thus, in Phase I, recognizing out-of-control data from the historical dataset accurately is important. In Phase II, the main concern is to detect process shifts from the baseline established in Phase I as quickly as possible when monitoring on-line data. Thus, to evaluate a monitoring scheme, the main concern in Phase I is to assess how effective the scheme can detect the out-of-control profiles correctly, while the emphasis of Phase II is on detecting process changes as quickly as possible. In Phase I, we will use the “true-alarm rate” (the rate of detecting real out-of-control profiles) and the “false-alarm rate” (the rate of claiming in-control profiles out of control) as our assessing criteria. In Phase II, the ARL is often used to compare the performances of competing control charts. We will also evaluate the performance of our Phase II method in terms of ARL.

If the parameters  $\alpha_0, \alpha_1, \sigma_0^2, \sigma_1^2$ , and  $\sigma_e^2$  are known, we can perform the Phase II operation directly. Our Phase II monitoring scheme of detecting shifts in the underlying parameters is a combined-chart scheme consisting of three univariate Shewhart-type control charts to monitor  $\alpha_0, \alpha_1$ , and  $\sigma_e^2$  separately.

Details are described in Subsection 3.4.

In practice, the values of the in-control parameters are unknown and must be estimated from a set of historical data collected from the process. If we have a set of in-control data, then we can estimate directly the parameter values; otherwise we need to perform a Phase I analysis to collect a set of in-control data. In this thesis, we provide two methods, the Bonferroni method and Multiple FDR method, to identify out-of-control profiles during Phase I. Details are described in Subsection 3.5.

### 3.3. Monitoring Statistics and their Distributions

For simplicity, we consider the case for which the  $x_i$ 's are fixed and take the same set of values for each profile. To avoid introducing new notation, we let the set points  $x_i$  be pre-coded so that  $\bar{x} = 0$  and still use the model (2) for our random-effect model. For the  $j^{\text{th}}$  linear profile, we estimate the intercept  $\alpha_{0j}$  and slope  $\alpha_{1j}$  by the least squares estimators. That is,

$$\hat{\alpha}_{0j} = \bar{y}_{\cdot j} \quad \text{and} \quad \hat{\alpha}_{1j} = \frac{S_{xy(j)}}{S_{xx}}, \quad (3)$$

where  $\bar{y}_{\cdot j} = \frac{1}{n} \sum_{i=1}^n y_{ij}$ ,  $S_{xy(j)} = \sum_{i=1}^n x_i (y_{ij} - \bar{y}_{\cdot j}) = \sum_{i=1}^n x_i y_{ij}$ , and  $S_{xx} = \sum_{i=1}^n x_i^2$ . And let

$$\hat{\sigma}_{ej}^2 = \frac{\sum_{i=1}^n (y_{ij} - \hat{y}_{ij})^2}{n-2} \quad (4)$$

be the estimator of the variance of  $\sigma_e^2$ , the error term of the  $j^{\text{th}}$  profile.

Assume there are  $k$  profiles in the historical dataset.

**Property 1.** Under the random-effect model (2) with coded  $x_i$ 's,

- (i)  $\hat{\alpha}_{01}, \dots, \hat{\alpha}_{0k}$  are i.i.d.  $N(\alpha_0, \sigma_0^2 + \frac{1}{n}\sigma_e^2)$ ,
- (ii)  $\hat{\alpha}_{11}, \dots, \hat{\alpha}_{1k}$  are i.i.d.  $N(\alpha_1, \sigma_1^2 + \frac{1}{S_{xx}}\sigma_e^2)$ ,
- (iii)  $\frac{(n-2)\hat{\sigma}_{e1}^2}{\sigma_e^2}, \dots, \frac{(n-2)\hat{\sigma}_{ek}^2}{\sigma_e^2}$  are i.i.d.  $\chi_{n-2}^2$ ,

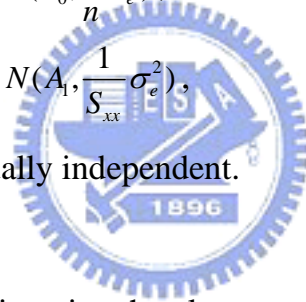
and these statistics are mutually independent.

Let  $\hat{A}_{0j}$  and  $\hat{A}_{1j}$  denote the least squares estimators of  $A_0$  and  $A_1$  for the  $j^{\text{th}}$  profile under the fixed-effect model (1) with coded  $x_i$ 's.

**Property 2.** Under the fixed-effect model (1) with coded  $x_i$ 's,

- (i)  $\hat{A}_{01}, \dots, \hat{A}_{0k}$  are i.i.d.  $N(A_0, \frac{1}{n}\sigma_e^2)$ ,
- (ii)  $\hat{A}_{11}, \dots, \hat{A}_{1k}$  are i.i.d.  $N(A_1, \frac{1}{S_{xx}}\sigma_e^2)$ ,

and these statistics are mutually independent.



Note the extra variation in the least squares estimators under the random-effect model, which can account for some uncontrollable common-cause variations. Thus, a monitoring scheme based on the random-effect model is a lot less sensitive to these common-cause variations than a scheme based on the fixed-effect model.

Let  $\eta_0^2 = \sigma_0^2 + \sigma_e^2/n$  and  $\eta_1^2 = \sigma_1^2 + \sigma_e^2/S_{xx}$ . Since  $\hat{\alpha}_{0j}$ 's are i.i.d.  $N(\alpha_0, \eta_0^2)$ , it is natural to estimate  $\alpha_0$  and  $\eta_0^2$  by the sample mean and sample variance of  $\{\hat{\alpha}_{0j}\}_{j=1}^k$  respectively.  $\alpha_1$  and  $\eta_1^2$  can be estimated in the same way. To estimate  $\sigma_e^2$ , simply take the average of  $\hat{\sigma}_{ej}^2$ 's. More specifically, we have

$$\hat{\alpha}_0 = \frac{1}{k} \sum_{j=1}^k \hat{\alpha}_{0j} \quad \text{and} \quad \hat{\eta}_0^2 = \frac{1}{k-1} \sum_{j=1}^k (\hat{\alpha}_{0j} - \hat{\alpha}_0)^2; \quad (5)$$

$$\hat{\alpha}_1 = \frac{1}{k} \sum_{j=1}^k \hat{\alpha}_{1j} \quad \text{and} \quad \hat{\eta}_1^2 = \frac{1}{k-1} \sum_{j=1}^k (\hat{\alpha}_{1j} - \hat{\alpha}_1)^2; \quad (6)$$

$$\hat{\sigma}_e^2 = \frac{\sum_{j=1}^k \sum_{i=1}^n (y_{ij} - \hat{y}_{ij})^2}{k(n-2)}, \quad \text{where} \quad \hat{y}_{ij} = \hat{\alpha}_{0j} + \hat{\alpha}_{1j} x_i. \quad (7)$$

We then have

**Property 3.** Under the random-effect model (2) with coded  $x_i$ 's,

- (i)  $\hat{\alpha}_0 \sim N(\alpha_0, \frac{1}{k} \eta_0^2)$ ,
- (ii)  $\hat{\alpha}_1 \sim N(\alpha_1, \frac{1}{k} \eta_1^2)$ ,
- (iii)  $(k-1)\hat{\eta}_0^2/\eta_0^2 \sim \chi_{k-1}^2$ ,
- (iv)  $(k-1)\hat{\eta}_1^2/\eta_1^2 \sim \chi_{k-1}^2$ ,
- (v)  $\frac{k(n-2)\hat{\sigma}_e^2}{\sigma_e^2} \sim \chi_{k(n-2)}^2$ ,



and these statistics are mutually independent.

In Phase I operation,  $\alpha_0$ ,  $\alpha_1$ ,  $\eta_0^2$ ,  $\eta_1^2$ , and  $\sigma_e^2$  are usually unknown. Hence, we substitute them by their estimators in the monitoring statistics. Thus the three monitoring statistics considered are  $(\hat{\alpha}_{0j} - \hat{\alpha}_0)^2 / \hat{\eta}_0^2$ ,  $(\hat{\alpha}_{1j} - \hat{\alpha}_1)^2 / \hat{\eta}_1^2$ , and  $\hat{\sigma}_{ej}^2 / \hat{\sigma}_e^2$ . To construct the control limits, we need their distributions. Denote the beta distribution with mean  $\alpha/(\alpha + \beta)$  by  $Beta(\alpha, \beta)$ .

**Property 4.** Under the random-effect model (2) with coded  $x_i$ 's,

- (i)  $\frac{k}{(k-1)^2} \frac{(\hat{\alpha}_{0j} - \hat{\alpha}_0)^2}{\hat{\eta}_0^2} \sim Beta(\frac{1}{2}, \frac{k-2}{2})$ ,

$$(ii) \frac{k}{(k-1)^2} \frac{(\hat{\alpha}_{1j} - \hat{\alpha}_1)^2}{\hat{\eta}_1^2} \sim \text{Beta} \left( \frac{1}{2}, \frac{k-2}{2} \right),$$

$$(iii) \frac{\hat{\sigma}_{ej}^2}{k\hat{\sigma}_e^2} \sim \text{Beta} \left( \frac{n-2}{2}, \frac{(k-1)(n-2)}{2} \right),$$

and these statistics are mutually independent.

All the proofs of the above properties are given in Appendix.

### 3.4. Phase II method

In Phase II, we assume that  $\alpha_0, \alpha_1, \sigma_0^2, \sigma_1^2$ , and  $\sigma_e^2$  are known. We adopt the combined-chart approach for profile monitoring. Set the overall false-alarm rate at  $\alpha$ . Since three charts are used simultaneously for process monitoring, we need to modify the individual false-alarm rate of each chart. By the fact that  $\hat{\alpha}_{0j}, \hat{\alpha}_{1j}$ , and  $\hat{\sigma}_{ej}^2$  are mutually independent, we can set the individual false-alarm rate of each chart at  $\alpha^* = 1 - (1 - \alpha)^{1/3}$  to achieve an overall false-alarm rate at  $\alpha$ . With  $\hat{\alpha}_{0j} \sim N(\alpha_0, \eta_0^2)$ ,  $\hat{\alpha}_{1j} \sim N(\alpha_1, \eta_1^2)$ , and

$$\frac{(n-2)\hat{\sigma}_{ej}^2}{\sigma_e^2} \sim \chi_{n-2}^2, \text{ we derive the control limits of the charts monitoring } \alpha_0, \alpha_1,$$

and  $\sigma_e^2$  as follows:

$$\begin{aligned} LCL_{\alpha_0} &= \alpha_0 - Z_{\alpha^*/2} \eta_0, & UCL_{\alpha_0} &= \alpha_0 + Z_{\alpha^*/2} \eta_0; \\ LCL_{\alpha_1} &= \alpha_1 - Z_{\alpha^*/2} \eta_1, & UCL_{\alpha_1} &= \alpha_1 + Z_{\alpha^*/2} \eta_1; \\ UCL_{\sigma_e^2} &= \frac{\sigma_e^2}{n-2} \chi_{\alpha^*, n-2}^2; \end{aligned} \tag{8}$$

where  $Z_{\alpha^*/2}$  is the  $(1-\alpha^*/2)\times 100$  percentile of the standard normal distribution and  $\chi_{\alpha^*,n-2}^2$  is the  $(1-\alpha^*)\times 100$  percentile of the Chi-square distribution of degrees of freedom  $n-2$ .

When the mean of  $A_{0j}$  shifts with a size of  $\delta\sigma_0$ ,  $\hat{\alpha}_{0j} \sim N(\alpha_0 + \delta\sigma_0, \eta_0^2)$ .

Let  $p_0$  be the probability that  $\hat{\alpha}_{0j}$  still falls within the control limits. Then

$$\begin{aligned} p_0 &= \Pr\{\alpha_0 - Z_{\alpha^*/2}\eta_0 \leq \hat{\alpha}_{0j} \leq \alpha_0 + Z_{\alpha^*/2}\eta_0\} \\ &= \Pr\left\{\frac{-\delta\sigma_0}{\eta_0} - Z_{\alpha^*/2} \leq \frac{\hat{\alpha}_{0j} - \alpha_0 - \delta\sigma_0}{\eta_0} \leq \frac{-\delta\sigma_0}{\eta_0} + Z_{\alpha^*/2}\right\} \\ &= \Phi\left(\frac{-\delta\sigma_0}{\eta_0} + Z_{\alpha^*/2}\right) - \Phi\left(\frac{-\delta\sigma_0}{\eta_0} - Z_{\alpha^*/2}\right). \end{aligned}$$

Similarly, when the mean of  $A_{1j}$  shifts from  $\alpha_1$  to  $\alpha_1 + \delta\sigma_1$ ,  $\hat{\alpha}_{1j} \sim N(\alpha_1 + \delta\sigma_1, \eta_1^2)$ . Then the probability that  $\hat{\alpha}_{1j}$  still falls within the control limits is

$$p_1 = \Phi\left(\frac{-\delta\sigma_1}{\eta_1} + Z_{\alpha^*/2}\right) - \Phi\left(\frac{-\delta\sigma_1}{\eta_1} - Z_{\alpha^*/2}\right).$$

Also, when the variance of  $\varepsilon_{ij}$  shifts from  $\sigma_e^2$  to  $(1+\delta)^2\sigma_e^2$ ,

$\frac{(n-2)\hat{\sigma}_{ej}^2}{(1+\delta)^2\sigma_e^2} \sim \chi_{n-2}^2$ . Then the probability  $p_e$  that  $\hat{\sigma}_{ej}^2$  still falls within the

control limits is given by

$$p_e = \Pr\left\{\frac{(n-2)\hat{\sigma}_{ej}^2}{(1+\delta)^2\sigma_e^2} \leq \frac{\chi_{\alpha^*,n-2}^2}{(1+\delta)^2}\right\} = F\left(\frac{\chi_{\alpha^*,n-2}^2}{(1+\delta)^2}\right),$$

where  $F$  is the cumulative distribution function (CDF) of the Chi-square distribution with  $n-2$  degrees of freedom. Note that  $p_0$ ,  $p_1$ , and  $p_e$  correspond to the probabilities of committing the type II error in testing hypothesis, respectively.



In Phase II operation, we adopt the combined-chart scheme in which the process signals out of control if any of the three statistics,  $\hat{\alpha}_{0j}, \hat{\alpha}_{1j}, \hat{\sigma}_{ej}^2$ , falls beyond the corresponding control limits. To evaluate the performance of the combined-chart scheme, we examine its run length distribution. The run length distribution is well known to be a geometric distribution with the “out-of-control probability”  $p$ , and  $p$  can be computed according to the process change. For example, if only the mean of  $A_{0j}$ ,  $\alpha_{0j}$ , shifts with the size described above, then  $p=1-p_0(1-\alpha)^{2/3}$ ; if  $\alpha_0$  and  $\alpha_1$  shift simultaneously, then  $p=1-p_0p_1(1-\alpha)^{1/3}$ , etc. Similarly, if the process is in control, then  $p=1-(1-\alpha)=\alpha$ . The ARL is the expectation of the run length distribution, which implies that  $ARL=1/p$ .

In Subsection 4.1.2, we will use simulation to verify the theoretical performance results mentioned above.

### 3.5. Phase I method

In practice, the in-control values of the process parameters are not known, so a major task in Phase I is to estimate them using historical data collected from the process. To detect out-of-control profiles among the  $k$  profiles in the historical dataset,  $k$  multiple tests are performed simultaneously. To control an overall false-alarm rate at level  $\alpha$ , we must adjust the false-alarm rate for each individual test. Here, we consider two methods, one is the commonly used Bonferroni method and the other is the Multiple FDR method proposed in this thesis.

### 3.5.1. Bonferroni method

Bonferroni inequality tells us that  $P(\bigcap_{j=1}^k E_j) \geq \sum_{j=1}^k P(E_j) - (k-1)$ , where  $E_j$ 's are any events. By rearranging terms, this becomes  $1 - P(\bigcap_{j=1}^k E_j) \leq k - \sum_{j=1}^k P(E_j)$ .

In our case,  $E_j$  represents the event that the  $j^{\text{th}}$  profile is in control. If we desire that the overall false-alarm rate is equal to or smaller than  $\alpha$ , then we must have  $1 - P(\bigcap_{j=1}^k E_j) \leq \alpha$ . If  $P(E_j) = 1 - \alpha/k$  for each  $j=1,2,\dots,k$ , then by Bonferroni Inequality,  $1 - P(\bigcap_{j=1}^k E_j) \leq k - \sum_{j=1}^k P(E_j) = k - k(1 - \alpha/k) = \alpha$ . Thus, if we control each individual false-alarm rate at level  $\alpha/k$ , then the overall false-alarm rate for the  $k$  profiles is controlled at level  $\alpha$ . We refer to this method as the Bonferroni method.

Moreover, in Phase I, we use three charts to monitor each profile simultaneously. Let the three monitoring statistics be

$$T_{0j} = \frac{(\hat{\alpha}_{0j} - \hat{\alpha}_0)^2}{\hat{\eta}_0^2}, \quad T_{1j} = \frac{(\hat{\alpha}_{1j} - \hat{\alpha}_1)^2}{\hat{\eta}_1^2}, \quad \text{and} \quad T_{ej} = \frac{\hat{\sigma}_{ej}^2}{\hat{\sigma}_e^2}. \quad (9)$$

Since  $T_{0j}$ ,  $T_{1j}$ , and  $T_{ej}$  are independent by Property 4, set the individual false-alarm rate of each chart at level  $\gamma = 1 - (1 - \alpha/k)^{1/3}$ . By Property 4, the control limits of  $T_{0j}$ ,  $T_{1j}$ , and  $T_{ej}$  are given respectively by

$$\begin{aligned} UCL_{T_{0j}} &= \frac{(k-1)^2}{k} \text{Beta}_{\gamma, \frac{1}{2}, \frac{k-2}{2}}, & UCL_{T_{1j}} &= \frac{(k-1)^2}{k} \text{Beta}_{\gamma, \frac{1}{2}, \frac{k-2}{2}}, \\ UCL_{T_{ej}} &= k \text{Beta}_{\gamma, \frac{n-2}{2}, \frac{(k-1)(n-2)}{2}}. \end{aligned} \quad (10)$$

Thus, with  $\gamma = 1 - (1 - \alpha/k)^{1/3}$ , we can control the overall false-alarm rate at level  $\alpha$ . We remark here that the Bonferroni method is well known to be fairly conservative in the sense that the actual false-alarm rate may be somewhat

smaller than the prescribed level  $\alpha$ .

### 3.5.2. Multiple FDR method

Extending the FDR-controlling method proposed by Benjamini and Hochberg (1995) to solving our problem, we propose a Multiple FDR method for Phase I monitoring. Note that in our case, we are not only facing the multiple-test problem, but also monitoring three statistics,  $T_{0j}$ ,  $T_{1j}$ , and  $T_{ej}$ , at the same time. For the  $j^{\text{th}}$  profile, we have three p-values:

$$p_{0j} = P(T_{0j} > t_{0j}), \quad p_{1j} = P(T_{1j} > t_{1j}), \quad p_{ej} = P(T_{ej} > t_{ej}), \quad (11)$$

where the lower-case letters,  $t_{0j}$ ,  $t_{1j}$ , and  $t_{ej}$ , denote the observed values of  $T_{0j}$ ,  $T_{1j}$ , and  $T_{ej}$ , respectively.

For the combined-chart scheme, it is easy to consider taking the minimum of the three p-values as its p-value since the combined-chart signals when any of the charts signals. Unfortunately, although the value of the minimum can be used to determine if the combined chart should signal out of control or not, it is not a p-value in nature.

Let  $F_0$ ,  $F_1$ , and  $F_e$  be the CDF of  $T_{0j}$ ,  $T_{1j}$ , and  $T_{ej}$ , respectively. Then, by (11), the minimum of the three p-values corresponding to the monitoring statistics  $T_{0j}$ ,  $T_{1j}$ , and  $T_{ej}$  is a random variable. Denote it by  $\tilde{P}_j$ . Then

$$\tilde{P}_j = \min(1 - F_0(T_{0j}), 1 - F_1(T_{1j}), 1 - F_e(T_{ej})) = \max(F_0(T_{0j}), F_1(T_{1j}), F_e(T_{ej})).$$

To derive the distribution of  $\tilde{P}_j$ , first note that  $F_0(T_{0j})$ ,  $F_1(T_{1j})$ ,  $F_e(T_{ej})$  are independent random variables uniformly distributed on the interval  $[0,1]$ .

Hence, the CDF of  $\tilde{P}_j$  is

$$\begin{aligned}
F_{\tilde{P}_j}(x) &= \Pr\{\tilde{P}_j \leq x\} = \Pr\{\max(F_0(T_{0j}), F_1(T_{1j}), F_e(T_{ej})) \leq x\} \\
&= \Pr\{F_0(T_{0j}) \leq x, F_1(T_{1j}) \leq x, F_e(T_{ej}) \leq x\} \\
&= \Pr\{F_0(T_{0j}) \leq x\} \cdot \Pr\{F_1(T_{1j}) \leq x\} \cdot \Pr\{F_e(T_{ej}) \leq x\} \\
&= x^3,
\end{aligned}$$

for  $x \in [0, 1]$ . Let  $\tilde{p}_j = \min(p_{0j}, p_{1j}, p_{ej})$ . Then the p-value corresponding to the  $j^{\text{th}}$  profile is then  $1 - \tilde{p}_j^3$ .

Let  $H_j, j=1, \dots, k$ , be the null hypothesis that the  $j^{\text{th}}$  profile is in control.

Based on the FDR procedure described before, we develop our Multiple FDR procedure as follows.

Step1. For the  $j^{\text{th}}$  profile, compute  $\hat{\alpha}_{0j}, \hat{\alpha}_{1j}, \hat{\sigma}_{ej}^2, j=1, \dots, k$ , by equations (3) and (4).

Step2. Compute  $\hat{\alpha}_0, \hat{\eta}_0^2, \hat{\alpha}_1, \hat{\eta}_1^2$ , and  $\hat{\sigma}_e^2$  by equations (5) – (7).

Step3. For  $j=1, \dots, k$ , compute  $t_{0j}, t_{1j}$ , and  $t_{ej}$  by equation (9) and their

corresponding p-values  $p_{0j}, p_{1j}$ , and  $p_{ej}$  by equation (11) and

Property 4.

Step4. For  $j=1, \dots, k$ , compute  $\tilde{p}_j = \min(p_{0j}, p_{1j}, p_{ej})$  and then  $p_j = 1 - \tilde{p}_j^3$ .

Let  $p_j$  be the corresponding p-value for testing the null hypothesis

$H_j, j=1, 2, \dots, k$ .

Step5. Let  $p_{(1)} \leq p_{(2)} \leq \dots \leq p_{(k)}$  be the ordered p-values. Let  $H_{(j)}$  be the

null hypothesis corresponding to  $p_{(j)}$ ,  $j=1, 2, \dots, k$ . Let  $l$  be the largest  $j$  for which  $p_{(j)} \leq \frac{j}{k} q^*$ , where  $q^*$  is the prescribed FDR level. If such  $l$  exists, reject all  $H_{(j)}$ ,  $j=1, 2, \dots, l$ ; otherwise, no hypotheses are rejected.

## 4. Simulation Results

In this section, the results of the simulation studies for Phase II and Phase I operations are summarized. For Phase II operation, the simulation study is simply to verify our theoretical results. For Phase I operation, we will compare the Multiple FDR method with the Bonferroni method in terms of the detecting power. The detecting power here is measured by the proportion of the out-of-control profiles being correctly rejected in each dataset. We refer to the expectation of this proportion as the “true-alarm rate”.

### 4.1. Phase II

#### 4.1.1. Settings

In our simulation study, we use an example similar to that used by Kang and Albin (2000) and Kim et. al (2003). In their simulation, they used the simple linear regression model:  $y_{ij} = 3 + 2x_i + \varepsilon_{ij}$ , where the  $\varepsilon_{ij}$ ’s are i.i.d. normal random variables with mean zero and variance one. We use the random-effect model (2) with  $\alpha_0 = 3$ ,  $\sigma_0^2 = 0.09$ ,  $\alpha_1 = 2$ ,  $\sigma_1^2 = 0.09$ ,  $\sigma_e^2 = 1$ ,  $n=50$ , and  $x_i = -24.5, -23.5, \dots, 23.5, 24.5$ .

Figure 1 shows 25 simulated profiles without error. The relationship between the response  $y_{ij}$  and the explanatory variable  $x_i$  is  $y_{ij} = A_{0j} + A_{1j}x_i$ , where  $A_{0j} \sim N(3, 0.09)$  and  $A_{1j} \sim N(2, 0.09)$ . Figure 2 shows 25 simulated profiles with error  $\varepsilon_{ij} \sim N(0, 1)$ .

We set the false-alarm rate  $\alpha = 0.0027$ , for which the in-control ARL is about 370 when the process is in control. For each situation under study, we simulate 50,000 profiles to obtain the proportion of the profiles being out-of-control. Then the ARL is estimated by the reciprocal of this proportion.

#### 4.1.2. Three Shewhart-type Control Charts

In Phase II operation, we use three Shewhart-type control charts to monitor  $\alpha_0, \alpha_1$ , and  $\sigma_{ej}^2$  separately.

With  $\alpha = 0.0027$  and  $n = 50$ , we have, by equation (8), the following control limits for the three charts:

$$LCL_{\alpha_0} = 1.898946, \quad UCL_{\alpha_0} = 4.101054;$$

$$LCL_{\alpha_1} = 1.003528, \quad UCL_{\alpha_1} = 2.996472;$$

$$UCL_{\sigma_e^2} = 1.759881.$$

The process signals out of control if any of the three estimators,  $\hat{\alpha}_{0j}$ ,  $\hat{\alpha}_{1j}$ ,  $\hat{\sigma}_{ej}^2$ , falls outside the control limits.

Table 2(a) shows the ARL performance when only the mean of the intercept term shifts from  $\alpha_0$  to  $\alpha_0 + \delta\sigma_0$ ,  $\delta = 0, 0.5, 1, \dots, 5$ . Table 2(b) shows the ARL performance when only the mean of the slope term shifts from  $\alpha_1$  to

$\alpha_1 + \delta \sigma_1$ ,  $\delta = 0, 0.5, 1, \dots, 5$ . Table 2(c) shows the ARL performance when only the standard deviation of error term shifts from  $\sigma_e$  to  $(1+\delta)\sigma_e$ ,  $\delta = 0, 0.05, 0.1, \dots, 0.5$ . The true ARL values in Tables 2(a)-2(c) are calculated by the method discussed in Subsection 3.4.

From Tables 2(a)-2(c), we find that the simulated ARLs are very close to the true ARLs, which verifies our theoretical results.

### 4.1.3. When the Fixed-effect Model is Mistakenly Used

For the fixed-effect model (1), the Phase II Shewhart-type control charts for monitoring  $A_0, A_1$ , and  $\sigma_e^2$  can be easily constructed by Property 2. Assume that the true values of  $A_0$  and  $A_1$  are  $\alpha_0$  and  $\alpha_1$  respectively. The control limits of  $A_0$  and  $A_1$  are given as follows:

$$LCL_{\alpha_0} = \alpha_0 - Z_{\alpha^*/2} \sigma_e / \sqrt{n}, \quad UCL_{\alpha_0} = \alpha_0 + Z_{\alpha^*/2} \sigma_e / \sqrt{n};$$

$$LCL_{\alpha_1} = \alpha_1 - Z_{\alpha^*/2} \sigma_e / \sqrt{S_{xx}}, \quad UCL_{\alpha_1} = \alpha_1 + Z_{\alpha^*/2} \sigma_e / \sqrt{S_{xx}};$$

$$UCL_{\sigma_e^2} = \frac{\sigma_e^2}{n-2} \chi_{\alpha^*, n-2}^2;$$

where  $\alpha^* = 1 - (1 - \alpha)^{1/3}$  and  $\alpha$  is the overall false-alarm rate for the combined chart.

What would happen if a process is of random effects and we monitor it as if it were of fixed effects?

Let  $\hat{\alpha}_{0j}$  and  $\hat{\alpha}_{1j}$  be the least squares estimators of the intercept and slope of the  $j^{\text{th}}$  profile respectively. Assuming the actual distribution of  $\hat{\alpha}_{0j}$  is  $N(\alpha_0, \eta_0^2)$ , the probability that  $\hat{\alpha}_{0j}$  still falls within the control limits

constructed based on the fixed-effect model (1) is given by

$$\begin{aligned}
p_{0f} &= \Pr(\alpha_0 - Z_{\alpha^*/2} \sigma_e / \sqrt{n} \leq \hat{\alpha}_{0j} \leq \alpha_0 + Z_{\alpha^*/2} \sigma_e / \sqrt{n}) \\
&= \Pr(-Z_{\alpha^*/2} \frac{\sigma_e / \sqrt{n}}{\eta_0} \leq \frac{\hat{\alpha}_{0j} - \alpha_0}{\eta_0} \leq Z_{\alpha^*/2} \frac{\sigma_e / \sqrt{n}}{\eta_0}) \\
&= \Phi(Z_{\alpha^*/2} \frac{\sigma_e / \sqrt{n}}{\eta_0}) - \Phi(-Z_{\alpha^*/2} \frac{\sigma_e / \sqrt{n}}{\eta_0}).
\end{aligned}$$

Similarly, for the slope, assuming the actual distribution of the slope estimator  $\hat{\alpha}_{1j}$  is  $N(\alpha_1, \eta_1^2)$ , the probability that  $\hat{\alpha}_{1j}$  still falls within the control limits is

$$p_{1f} = \Phi(Z_{\alpha^*/2} \frac{\sigma_e / \sqrt{S_{xx}}}{\eta_1}) - \Phi(-Z_{\alpha^*/2} \frac{\sigma_e / \sqrt{S_{xx}}}{\eta_1}).$$

Assume that  $\hat{\alpha}_{0j} \sim N(\alpha_0, \eta_0^2)$  and  $\hat{\alpha}_{1j} \sim N(\alpha_1, \eta_1^2)$ . If we monitor the process using the above fixed-effect control limits, then the overall false-alarm rate is  $p_f^* = 1 - p_{0f} \cdot p_{1f} \cdot \sqrt[3]{1 - \alpha}$ . Hence, the run length distribution is Geometric ( $p_f^*$ ), which implies  $ARL = 1/p_f^*$ . For the example described before, Table 3 presents the control limits for both the random-effect and fixed-effect model and their in-control ARL (denoted by  $ARL_0$ ).

From Table 3,  $ARL_0$  is 370.37037 when the correct model is employed, but dramatically drops down to 1.078406 when the fixed-effect model is mistakenly used. We can see that, for our example, the process is of random effects, but when monitored with the fixed-effect model, it results in incredibly many false alarms! (92.73% are false alarms!) We remark that in calculating  $p_{0f}$  and  $p_{1f}$ , we plug in the true values of  $\sigma_e, \eta_0, \eta_1$ , and  $S_{xx}$ . In reality, when a fixed-effect model is mistakenly used, the profile-to-profile variation is



considered as part of the random error represented by  $\varepsilon_{ij}$ . Thus  $\sigma_e$  is inflated by the extra variation. If  $\sigma_e$  needs to be estimated from a set of Phase I data, as it often does, we can consider

$$\hat{\sigma}_e^2 = \frac{1}{(nk - 2)} \sum_{j=1}^k \sum_{i=1}^n (y_{ij} - \hat{A}_0 - \hat{A}_1 x_i)^2, \quad (12)$$

where  $\hat{A}_0 = \frac{1}{kn} \sum_{j=1}^k \sum_{i=1}^n y_{ij} = \frac{1}{k} \sum_{j=1}^k \bar{y}_{\cdot j}$  and  $\hat{A}_1 = \frac{\sum_{j=1}^k S_{xy(j)}}{\sum_{j=1}^k S_{xx}} = \frac{1}{k S_{xx}} \sum_{j=1}^k S_{xy(j)}$  are respectively the least squares estimators under the fixed-effect model (1).

To study the  $ARL_0$  behavior of such case, we conduct a simulation study. For  $k=100$ ,  $n=50$ , we generate 50,000 sets of linear profile data under the random-effect model (2) as before. For each dataset, we obtain  $\hat{\sigma}_e^2$  by equation (12), and calculate  $ARL_0$  as described above with  $\sigma_e$  replaced by  $\hat{\sigma}_e$ . We then compute the sample mean and sample standard deviation of these 50,000  $ARL_0$  values. The average of the 50,000  $\hat{\sigma}_e$ 's is also calculated. We obtain an estimate of  $ARL_0$ ,  $\hat{ARL}_0 = 1.584157$ , with standard error 0.000258. The average  $\hat{\sigma}_e$  is 4.424026, inflated from  $\sigma_e=1$  by the profile-to-profile variation. However, this does not account enough for the extra variation since the average  $ARL_0$  only increases from 1.078406 to 1.584157, which is still very far off from the designed value 370.37 (i.e., 63.13% are false alarms).

We also observe that if we monitor the process using the correct random-effect model, the choice of the covariate  $x_i$ 's will not affect the  $ARL_0$  performance, but not so for using a fixed-effect model mistakenly. Table 4 shows that when the range of  $x_i$ 's gets narrower, the false alarms get fewer,

but the  $ARL_0$  is still too far off from the designed value 370.37.

## 4.2. Phase I

For Phase I methods, we compare the Multiple FDR method with the Bonferroni method in terms of their true-alarm rates. For each case under study, we repeat 10000 times to estimate the true-alarm rate, the expected proportion of the out-of-control profiles being correctly detected. Again, we consider the profile is out of control if any of the three control charts signals.

The setting of the simulation study is the same as that for Phase II. For the Bonferroni method, we set the overall false-alarm rate at  $\alpha=0.05$ . For the Multiple FDR method, we set the FDR at  $q^* = 0.05$  as well. In Phase I study, we need to generate sets of historical data.

In our simulation, a historical dataset consists of 50 profiles, in which we set one, two, or three out-of-control profiles. The scenarios of the out-of-control processes are the same as that for the Phase II study. For  $\alpha=0.05$  and  $k=50$ , the control limits of  $T_{0j}$ ,  $T_{1j}$ , and  $T_{ej}$  are given below:

$$UCL_{T_{0j}}=11.39625, \quad UCL_{T_{1j}}=11.39625, \text{ and } UCL_{T_{ej}}=1.8295.$$

With our monitoring scheme, calculate the proportion of the correct alarms within the true out-of-control profiles. Repeat this 10000 times and calculate the averaged proportion of the correct alarms. This averaged proportion is an estimate of the “true-alarm rate”. Similarly, we can obtain an estimate of the “false-alarm rate” by averaging 10000 sample proportions of the false alarms within the in-control historical profiles.

For both Bonferroni method and Multiple FDR method, Tables 5-7 present the true-alarm rate and false-alarm rate for shifts in  $\alpha_0$ ,  $\alpha_1$ , and  $\sigma_e^2$  respectively. And the results for the cases of one, two, and three out-of-control profiles are given in subtables (a), (b), (c) respectively. Figures 3-5 show the true-alarm rate comparisons of the two methods for  $\alpha_0$ ,  $\alpha_1$ , and  $\sigma_e^2$  shifts respectively.

From these Tables and Figures, we observe the followings.

- More out-of-control profiles in historical data leads to lower detecting powers.
- The Multiple FDR method is generally better than the Bonferroni method in terms of the true-alarm rate. The gain in power tends to be larger for more out-of-control profiles in historical data. However, we have to admit that the gain by using the FDR approach is fairly limited.

Figures 6-8 show the comparison results by the false-alarm rate respectively for shifts in  $\alpha_0$ ,  $\alpha_1$ , and  $\sigma_e^2$ . From these figures, we can clearly see the price that the Multiple FDR method pays for getting better detecting power. However, although the false-alarm rate of the Multiple FDR method is larger than that of the Bonferroni method, the size of the rate is still fairly small (all less than 0.003).

It may seem that the power is not promising since the power does not exceed 0.9 until the mean of the intercept (or slope) term shifts by about  $6\sigma_0$  (or  $5.5\sigma_1$ ) for the case of one out-of-control profile. This result is somewhat disappointing. To figure out why the power is so low, we compare it with that of the individual X chart for Phase I operation.

Table 8 shows the power of the individual X chart in Phase I with  $\alpha = 0.05$  and  $k=50$ , where  $\alpha$  is the overall false-alarm rate and  $k$  is the number of data points in the historical dataset. The power  $p$  in the table is obtained by calculating  $p = 1 - \Phi(-\delta + Z_{\alpha/2k}) + \Phi(-\delta - Z_{\alpha/2k})$ , which is the probability of a normal random variable  $X$  lies outside the control limits  $[\mu - Z_{\alpha/2k}\sigma, \mu + Z_{\alpha/2k}\sigma]$  when the mean has shifted from  $\mu$  to  $\mu + \delta\sigma$ . We can see that the power of the individual X chart does not exceed 0.9 until  $\delta=5$ . Hence, the power of our Phase I scheme under random-effects is not too disappointing when compared with the individual X chart. The low power simply is the effect of the multiple-test problem. With  $\alpha = 0.05$  and  $k=50$ ,  $\alpha/k=0.001$ , which is a lot smaller than the regular 3-sigma level at 0.0027. Thus, in real-life applications, if we want to have a better power for detecting out-of-control profiles in Phase I, a simple remedy is to allow a higher overall false-alarm rate  $\alpha$ . After all, setting  $\alpha=0.05$  for comparison studies is simply a choice of convenience.

## 5. Conclusion

Profile monitoring is a field of much interest recently. Most studies are based on fixed-effect models. In this thesis, we introduce a linear profile monitoring with a random-effect model to allow more common-cause variations in the system and hence reducing unnecessary false alarms. Our simulation study demonstrates that, if the process is of random effects but we mistakenly monitor it with a fixed-effect model, incredibly many false alarms will occur.

In Phase II monitoring, instead of the three EWMA charts proposed by Kim et al. (2003), we use three independent Shewhart-type charts. We distribute the same individual in-control false-alarm rate to each chart to achieve the overall false-alarm rate at level  $\alpha$ . In Phase I monitoring, for each individual chart, estimators across profiles are not independent. But the three estimators  $(\hat{\alpha}_{0j}, \hat{\alpha}_{1j}, \hat{\sigma}_{ej}^2)$  for the same profile are independent. Therefore, to control the FWER in Phase I monitoring, the Bonferroni method and the Multiple FDR method are implemented and compared. The Multiple FDR method is better than the Bonferroni method in terms of the true-alarm rate, especially when more out-of-control profiles exist in the historical data. The tradeoff is the slightly increased false-alarm rate. So, in Phase I monitoring, we recommend using Multiple FDR method to detect out-of-control profiles from the historical profile data.

In this work, we have monitored the shift of the mean of intercept term ( $\alpha_0$ ), the shift of the mean of slope term ( $\alpha_1$ ), and the change of the variance of error term ( $\sigma_e^2$ ). But the variance of intercept term ( $\sigma_0^2$ ) and the variance of slope term ( $\sigma_1^2$ ) can not be monitored when only one profile is observed at each time point. If rational subgroups of profiles are available for the process, then it is feasible to monitor the variance of the intercept and slope in the random-effect model. Developing an adequate monitoring scheme for such process is a potential future research topic.

## 6. Appendix

### Proof of Property 1.

(i) Since  $\hat{\alpha}_{0j} = \bar{y}_{\cdot j}$  and  $\sum_{i=1}^n x_i = 0$ , we have

$$\hat{\alpha}_{0j} = \frac{1}{n} \sum_{i=1}^n (A_{0j} + A_{1j}x_i + \varepsilon_{ij}) = \frac{1}{n} (nA_{0j} + A_{1j} \sum_{i=1}^n x_i + \sum_{i=1}^n \varepsilon_{ij}) = A_{0j} + \frac{1}{n} \sum_{i=1}^n \varepsilon_{ij}. \quad (\text{A1})$$

Thus,  $E(\hat{\alpha}_{0j}) = \alpha_0$  and  $\text{Var}(\hat{\alpha}_{0j}) = \sigma_0^2 + \frac{1}{n} \sigma_e^2$ .

Therefore,  $\hat{\alpha}_{0j} \sim N(\alpha_0, \sigma_0^2 + \frac{1}{n} \sigma_e^2)$ .

(ii) Since  $\hat{\alpha}_{1j} = S_{xy(j)} / S_{xx}$ , we have

$$\begin{aligned} \hat{\alpha}_{1j} &= \frac{1}{S_{xx}} \sum_{i=1}^n x_i y_{ij} = \frac{1}{S_{xx}} \sum_{i=1}^n x_i (A_{0j} + A_{1j}x_i + \varepsilon_{ij}) \\ &= \frac{1}{S_{xx}} \left( A_{1j} S_{xx} + \sum_{i=1}^n x_i \varepsilon_{ij} \right) = A_{1j} + \frac{1}{S_{xx}} \sum_{i=1}^n x_i \varepsilon_{ij}. \end{aligned} \quad (\text{A2})$$

Thus,  $E(\hat{\alpha}_{1j}) = \alpha_1$  and  $\text{Var}(\hat{\alpha}_{1j}) = \sigma_1^2 + \frac{1}{S_{xx}^2} \sum_{i=1}^n x_i^2 \text{Var}(\varepsilon_{ij}) = \sigma_1^2 + \frac{1}{S_{xx}} \sigma_e^2$ .

Therefore,  $\hat{\alpha}_{1j} \sim N(\alpha_1, \sigma_1^2 + \frac{1}{S_{xx}} \sigma_e^2)$ .

(iii) It is well known (Theorem 6.2.1, Graybill (1976)) that

$$(n-2)\hat{\sigma}_{ej}^2 / \sigma_e^2 \sim \chi_{n-2}^2, \text{ for each } j=1, \dots, k.$$

The mutual independence of the statistics are obvious since  $\hat{\alpha}_{0j}$ ,  $\hat{\alpha}_{1j}$ , and  $\hat{\sigma}_{ej}^2$  are independent for each  $j$ .

### Proof of Property 2.

Similar to (A1) and (A2), we have

$$\hat{A}_{0j} = A_0 + \frac{1}{n} \sum_{i=1}^n \varepsilon_{ij} \quad \text{and} \quad \hat{A}_{1j} = A_1 + \frac{1}{S_{xx}} \sum_{i=1}^n x_i \varepsilon_{ij}.$$

Thus,  $E(\hat{A}_{0j}) = A_0$  and  $Var(\hat{A}_{0j}) = \frac{1}{n} \sigma_e^2$ ;  $E(\hat{A}_{1j}) = A_1$  and  $Var(\hat{A}_{1j}) = \frac{1}{S_{xx}} \sigma_e^2$ .

Therefore,  $\hat{A}_{0j} \sim N(A_0, \frac{1}{n} \sigma_e^2)$  and  $\hat{A}_{1j} \sim N(A_1, \frac{1}{S_{xx}} \sigma_e^2)$ .

### Proof of Property 3.

(i) – (iv) are well known results for i.i.d. normal variates. To prove (v), since  $k(n-2)\hat{\sigma}_e^2/\sigma_e^2$  is the sum of  $k$  independent  $\chi_{n-2}^2$  variates, it is distributed as  $\chi_{k(n-2)}^2$ . The independence property is also obvious by Property 1 and by the well-known fact that the sample mean and sample variance of i.i.d. normal variates are independent. And by the independence of  $\hat{\alpha}_{0j}$ 's,  $\hat{\alpha}_{1j}$ 's, and  $\hat{\sigma}_{ej}^2$ 's, the mutual independence of  $\hat{\alpha}_0, \hat{\alpha}_1, \hat{\eta}_0^2, \hat{\eta}_1^2$ , and  $\hat{\sigma}_e^2$  holds.

### Proof of Property 4.

(i) By Property 1,  $\hat{\alpha}_{0j}$  are i.i.d.  $N(\alpha_0, \eta_0^2)$ ,  $j=1, \dots, k$ . Since  $\hat{\alpha}_0$  and  $\hat{\eta}_0^2$  are sample mean and variance of  $\{\hat{\alpha}_{0j}\}$ , respectively, we have

$$\hat{\alpha}_0 \sim N(\alpha_0, \eta_0^2/k) \quad \text{and} \quad (k-1)\hat{\eta}_0^2/\eta_0^2 \sim \chi_{k-1}^2. \quad \text{Let } Y_1 = (k/k-1)(\hat{\alpha}_{0j} - \hat{\alpha}_0)^2/\eta_0^2$$

$$\text{and } Y_2 = (k-1)\hat{\eta}_0^2/\eta_0^2. \quad \text{Then } Y_1 \sim \chi_1^2, \text{ and } Y_2 \sim \chi_{k-1}^2. \quad \text{Let } Y_3 = Y_2 - Y_1.$$

$$\text{Then } Y_3 = \left[ \frac{1}{\eta_0^2} \left( \sum_{l=1}^k (\hat{\alpha}_{0l} - \hat{\alpha}_0)^2 - \frac{k}{k-1} (\hat{\alpha}_{0j} - \hat{\alpha}_0)^2 \right) \right].$$

By Cochran's Theorem (see Casella and Berger (2002), Page 536-537),

$Y_1$  is independent of  $Y_3$ . Hence,


$$\frac{k}{(k-1)^2} \frac{(\hat{\alpha}_{0j} - \hat{\alpha}_0)^2}{\hat{\eta}_0^2} = \frac{Y_1}{Y_1 + Y_3} \sim \text{Beta}\left(\frac{1}{2}, \frac{k-2}{2}\right).$$

(ii) Similarly, we can derive that  $\frac{k}{(k-1)^2} \frac{(\hat{\alpha}_{1j} - \hat{\alpha}_1)^2}{\hat{\eta}_1^2} \sim \text{Beta}\left(\frac{1}{2}, \frac{k-2}{2}\right).$

(iii) We have proved that  $\frac{(n-2)\hat{\sigma}_{ej}^2}{\sigma_e^2} \sim \chi_{n-2}^2$  and  $\frac{k(n-2)\hat{\sigma}_e^2}{\sigma_e^2} \sim \chi_{k(n-2)}^2$ . Again,

$$\text{by Cochran's theorem, } \frac{\hat{\sigma}_{ej}^2}{k\hat{\sigma}_e^2} = \frac{\frac{(n-2)\hat{\sigma}_{ej}^2}{\sigma_e^2}}{\frac{k(n-2)\hat{\sigma}_e^2}{\sigma_e^2}} \sim \text{Beta}\left(\frac{n-2}{2}, \frac{(k-1)(n-2)}{2}\right).$$

## 7. References

- 
- [1] Benjamini, Y. and Hochberg, Y. (1995). "Controlling the False Discovery Rate: a Practical and Powerful Approach to Multiple Testing". *J. R. Statist. Soc. B*, 57, 1, 289-300.
- [2] Casella, G. and Berger, R. L. (2002). *Statistical Inference*. 2<sup>nd</sup> Edition, Duxbury.
- [3] DeVor, R. E., Chang, T., and Sutherland, J. W. (1992). *Statistical Quality Design and Control: Contemporary Concepts and Methods*. Macmillan, New York.
- [4] Graybill, F. A. (1976). *Theory and Application of the Linear Model*, Duxbury, Massachusetts.
- [5] Kang, L and Albin, S. L. (2000). "On-line Monitoring When the Process Yields a Linear Profile". *Journal of Quality Technology*, 32, 418-426.



- [6] Kim, K., Mahmoud, M. A., and Woodall, W. H. (2003). "On The Monitoring of Linear Profiles". *Journal of Quality Technology*, 35, 3, 317-328.
- [7] Mahmoud, M. A. and Woodall, W. H. (2004). "Phase I Analysis of Linear Profiles With Calibration Applications". *Technometrics*, 46, 4, 380-391.
- [8] Mahmoud, M. A. (2004). "The Monitoring of Linear Profiles and the Inertial Properties of Control Charts". Ph.D. Thesis, the Virginia Polytechnic Institute and State University.
- [9] Montgomery, D. C. (2005). *Introduction to Statistical Quality Control*. 5<sup>th</sup> Edition. John Wiley & Sons, New York.
- [10] Shiau, J.-J. H. and Weng, Z.-P. (2004). "Profile Monitoring by Nonparametric Regression". Technical Report. NSC92-2118-M-009-012. To be submitted.



## Tables

Table 1. Possible outcomes of testing  $k$  hypotheses.

	Declared non-significant	Declared significant	Total
True null hypotheses	$k_0 - R_0$	$R_0$	$k_0$
Non-true null hypotheses	$k_1 - R_1$	$R_1$	$k_1$
Total	$k - R$	$R$	$k$



Table 2(a). The ARL performance when the mean of the intercept term shifts from  $\alpha_0$  to  $\alpha_0 + \delta\sigma_0$ ,  $\delta=0, 0.5, 1, \dots, 5$ ,  $\sigma_0=0.3$ .

$\delta$	True ARL	Simulated ARL
0	370.3704	373.3181
0.5	253.4116	254.4916
1	103.5233	103.9755
1.5	37.6245	37.6068
2	14.9016	14.9010
2.5	6.8281	6.8287
3	3.6564	3.6564
3.5	2.2736	2.2739
4	1.6183	1.6180
4.5	1.2921	1.2919
5	1.1291	1.1291

Table 2(b). The ARL performance when the mean of slope term shifts from  $\alpha_1$  to  $\alpha_1 + \delta\sigma_1$ ,  $\delta=0, 0.5, 1, \dots, 5$ ,  $\sigma_1=0.3$ .

$\delta$	True ARL	Simulated ARL
0	370.3704	372.6310
0.5	234.5383	235.3724
1	83.6770	83.7613
1.5	27.7234	27.6989
2	10.5374	10.5382
2.5	4.8261	4.8276
3	2.6662	2.6657
3.5	1.7497	1.7500
4	1.3305	1.3304
4.5	1.1354	1.1353
5	1.0489	1.0489

Table 2(c). The ARL performance when the standard deviation of the error term shifts from  $\sigma_e$  to  $(1+\delta)\sigma_e$ ,  $\delta=0, 0.05, 0.1, \dots, 0.5$ ,  $\sigma_e=1$ .

$\delta$	True ARL	Simulated ARL
0	370.3782	372.3441
0.05	139.2531	137.5285
0.1	42.9459	42.6163
0.15	15.6391	15.5591
0.2	7.1022	7.0846
0.25	3.9165	3.9099
0.3	2.5282	2.5252
0.35	1.8469	1.8454
0.4	1.4835	1.4825
0.45	1.2790	1.2783
0.5	1.1605	1.1601

Table 3.  $ARL_0$  performance when  $\hat{\alpha}_{0j} \sim N(\alpha_0, \eta_0^2)$  and  $\hat{\alpha}_{1j} \sim N(\alpha_1, \eta_1^2)$ ,

but monitored with the fixed-effect model (1)

	Random-Effect (correct)	Fixed-Effect (misused) ( $\sigma_e^2 = 1$ )
Upper control limit of $\hat{\alpha}_{0j}$	4.101054	3.469491
Lower control limit of $\hat{\alpha}_{0j}$	1.898946	2.530509
Upper control limit of $\hat{\alpha}_{1j}$	2.996472	2.032534
Lower control limit of $\hat{\alpha}_{1j}$	1.003528	1.967466
Upper control limit of $\hat{\sigma}_{ej}^2$	1.759881	1.759881
$ARL_0$	370.370370	1.078406

Table 4.  $ARL_0$  performance under different covariate ( $x_i$ ) choices when the fixed-effect model is mistakenly used

The range of $x_i$ 's	$ARL_0$
$x_i = -24.5, -23.5, \dots, 24.5$	1.078405882
$x_i = -4.5, -3.5, \dots, 4.5$	1.397040407
$x_i = -0.45, -0.35, \dots, 0.45$	5.399986423

Table 5(a). The true-alarm rate and false-alarm rate when the mean of the intercept term shifts from  $\alpha_0$  to  $\alpha_0 + \delta\sigma_0$ ,  $\delta = 0, 0.5, 1, \dots, 10$ ,  $\sigma_0 = 0.3$ , for the case of one out-of-control profile.

True-alarm rate			False-alarm rate		
$\delta$	Bonferroni Method	Multiple FDR Method	$\delta$	Bonferroni Method	Multiple FDR Method
0			0	0.001076	0.001152
0.5	0.0017	0.0024	0.5	0.000976	0.001076
1	0.0035	0.0045	1	0.000978	0.001045
1.5	0.0108	0.0087	1.5	0.000833	0.000969
2	0.0294	0.0270	2	0.000922	0.000941
2.5	0.0670	0.0723	2.5	0.000804	0.001012
3	0.1399	0.1437	3	0.000812	0.000941
3.5	0.2566	0.2604	3.5	0.000759	0.001057
4	0.4062	0.4066	4	0.000710	0.001094
4.5	0.5717	0.5746	4.5	0.000761	0.001190
5	0.7224	0.7229	5	0.000682	0.001282
5.5	0.8472	0.8558	5.5	0.000682	0.001380
6	0.9212	0.9244	6	0.000684	0.001349
6.5	0.9667	0.9693	6.5	0.000608	0.001439
7	0.9860	0.9892	7	0.000722	0.001396
7.5	0.9970	0.9963	7.5	0.000669	0.001316
8	0.9992	0.9995	8	0.000671	0.001469
8.5	0.9997	0.9997	8.5	0.000737	0.001363
9	1.0000	1.0000	9	0.000622	0.001367
9.5	1.0000	1.0000	9.5	0.000724	0.001400
10	1.0000	1.0000	10	0.000688	0.001396

Table 5(b). The true-alarm rate and false-alarm rate when the mean of the intercept term shifts from  $\alpha_0$  to  $\alpha_0 + \delta\sigma_0$ ,  $\delta = 0, 0.5, 1, \dots, 10$ ,  $\sigma_0 = 0.3$ , for the case of two out-of-control profiles.

True-alarm rate			False-alarm rate		
$\delta$	Bonferroni Method	Multiple FDR Method	$\delta$	Bonferroni Method	Multiple FDR Method
0			0	0.001016	0.001088
0.5	0.00145	0.00145	0.5	0.000921	0.001090
1	0.00330	0.00295	1	0.000975	0.001027
1.5	0.00920	0.00990	1.5	0.000921	0.000990
2	0.01995	0.02275	2	0.000867	0.000954
2.5	0.04400	0.04515	2.5	0.000819	0.000904
3	0.08480	0.08755	3	0.000706	0.000965
3.5	0.14870	0.15650	3.5	0.000610	0.001102
4	0.23005	0.25075	4	0.000735	0.001165
4.5	0.32205	0.36810	4.5	0.000615	0.001296
5	0.43030	0.49030	5	0.000667	0.001463
5.5	0.54135	0.61485	5.5	0.000635	0.001602
6	0.64095	0.72520	6	0.000642	0.001783
6.5	0.73250	0.80985	6.5	0.000619	0.001771
7	0.80285	0.87685	7	0.000627	0.001962
7.5	0.86225	0.91955	7.5	0.000733	0.001942
8	0.90865	0.95110	8	0.000665	0.001965
8.5	0.93985	0.97065	8.5	0.000604	0.002144
9	0.96310	0.98400	9	0.000652	0.002002
9.5	0.97730	0.99060	9.5	0.000667	0.002152
10	0.98555	0.99510	10	0.000685	0.002015

Table 5(c). The true-alarm rate and false-alarm rate when the mean of the intercept term shifts from  $\alpha_0$  to  $\alpha_0 + \delta\sigma_0$ ,  $\delta = 0, 0.5, 1, \dots, 10$ ,  $\sigma_0 = 0.3$ , for the case of three out-of-control profiles.

True-alarm rate			False-alarm rate		
$\delta$	Bonferroni Method	Multiple FDR Method	$\delta$	Bonferroni Method	Multiple FDR Method
0			0	0.001008	0.001100
0.5	0.00160	0.00113	0.5	0.000966	0.000991
1	0.00253	0.00277	1	0.000915	0.001004
1.5	0.00667	0.00707	1.5	0.000781	0.000945
2	0.01387	0.01513	2	0.000819	0.000915
2.5	0.02980	0.03050	2.5	0.000694	0.000879
3	0.05033	0.05190	3	0.000726	0.000877
3.5	0.08163	0.08563	3.5	0.000679	0.000877
4	0.11537	0.12960	4	0.000645	0.001121
4.5	0.16207	0.18987	4.5	0.000634	0.001279
5	0.20877	0.25657	5	0.000660	0.001360
5.5	0.26347	0.33640	5.5	0.000657	0.001617
6	0.31707	0.42140	6	0.000655	0.001755
6.5	0.37157	0.50837	6.5	0.000657	0.002021
7	0.42877	0.58943	7	0.000732	0.002115
7.5	0.47950	0.66373	7.5	0.000694	0.002168
8	0.53577	0.72467	8	0.000732	0.002145
8.5	0.58503	0.78327	8.5	0.000679	0.002494
9	0.62607	0.82310	9	0.000760	0.002583
9.5	0.67087	0.86197	9.5	0.000643	0.002617
10	0.70707	0.89047	10	0.000649	0.002681

Table 6(a). The true-alarm rate and false-alarm rate when the mean of the slope term shifts from  $\alpha_1$  to  $\alpha_1 + \delta\sigma_1$ ,  $\delta=0, 0.5, 1, \dots, 10$ ,  $\sigma_1=0.3$ , for the case of one out-of-control profile.

True-alarm rate			False-alarm rate		
$\delta$	Bonferroni Method	Multiple FDR Method	$\delta$	Bonferroni Method	Multiple FDR Method
0			0	0.000958	0.001136
0.5	0.0013	0.0021	0.5	0.000939	0.001082
1	0.0046	0.0048	1	0.000984	0.001049
1.5	0.0133	0.0151	1.5	0.000971	0.000978
2	0.0430	0.0440	2	0.000880	0.001006
2.5	0.1007	0.1032	2.5	0.000800	0.001002
3	0.2101	0.2100	3	0.000780	0.001002
3.5	0.3672	0.3662	3.5	0.000796	0.001143
4	0.5383	0.5515	4	0.000722	0.001161
4.5	0.7134	0.7267	4.5	0.000712	0.001333
5	0.8472	0.8527	5	0.000669	0.001384
5.5	0.9319	0.9339	5.5	0.000678	0.001402
6	0.9735	0.9740	6	0.000684	0.001502
6.5	0.9923	0.9906	6.5	0.000608	0.001343
7	0.9973	0.9981	7	0.000641	0.001386
7.5	0.9995	0.9993	7.5	0.000704	0.001420
8	0.9998	1.0000	8	0.000692	0.001400
8.5	1.0000	1.0000	8.5	0.000598	0.001353
9	1.0000	1.0000	9	0.000737	0.001408
9.5	1.0000	1.0000	9.5	0.000720	0.001367
10	1.0000	1.0000	10	0.000669	0.001404



Table 6(b) The true-alarm rate and false-alarm rate when the mean of the slope term shifts from  $\alpha_1$  to  $\alpha_1 + \delta\sigma_1$ ,  $\delta=0, 0.5, 1, \dots, 10$ ,  $\sigma_1=0.3$ , for the case of two out-of-control profiles.

True-alarm rate			False-alarm rate		
$\delta$	Bonferroni Method	Multiple FDR Method	$\delta$	Bonferroni Method	Multiple FDR Method
0			0	0.001016	0.001148
0.5	0.00205	0.00080	0.5	0.000983	0.001052
1	0.00355	0.00495	1	0.000921	0.000992
1.5	0.01035	0.01145	1.5	0.000921	0.000963
2	0.03060	0.02910	2	0.000829	0.000923
2.5	0.06425	0.06425	2.5	0.000748	0.000910
3	0.12110	0.12645	3	0.000715	0.001115
3.5	0.20580	0.22405	3.5	0.000648	0.001106
4	0.30475	0.33580	4	0.000665	0.001294
4.5	0.42920	0.48980	4.5	0.000717	0.001540
5	0.53965	0.61900	5	0.000629	0.001621
5.5	0.65550	0.73510	5.5	0.000629	0.001765
6	0.75215	0.82665	6	0.000635	0.001848
6.5	0.82535	0.89175	6.5	0.000685	0.001988
7	0.88945	0.93615	7	0.000619	0.002048
7.5	0.92990	0.96145	7.5	0.000725	0.002058
8	0.95525	0.98070	8	0.000658	0.001967
8.5	0.97440	0.98975	8.5	0.000621	0.002144
9	0.98590	0.99390	9	0.000708	0.002006
9.5	0.99300	0.99775	9.5	0.000671	0.002131
10	0.99655	0.99935	10	0.000704	0.002194

Table 6(c). The true-alarm rate and false-alarm rate when the mean of the slope term shifts from  $\alpha_1$  to  $\alpha_1 + \delta\sigma_1$ ,  $\delta=0, 0.5, 1, \dots, 10$ ,  $\sigma_1=0.3$ , for the case of three out-of-control profiles.

True-alarm rate			False-alarm rate		
$\delta$	Bonferroni Method	Multiple FDR Method	$\delta$	Bonferroni Method	Multiple FDR Method
0			0	0.000942	0.001070
0.5	0.00157	0.00123	0.5	0.001006	0.001102
1	0.00367	0.00430	1	0.000909	0.000964
1.5	0.00907	0.00900	1.5	0.000828	0.000883
2	0.02050	0.02057	2	0.000796	0.000838
2.5	0.03953	0.04003	2.5	0.000791	0.000864
3	0.06667	0.07660	3	0.000691	0.001009
3.5	0.10543	0.11983	3.5	0.000704	0.001130
4	0.15147	0.17710	4	0.000685	0.001160
4.5	0.20677	0.25303	4.5	0.000679	0.001357
5	0.26947	0.33440	5	0.000730	0.001483
5.5	0.32667	0.43323	5.5	0.000660	0.001796
6	0.39177	0.52567	6	0.000621	0.002060
6.5	0.44757	0.61897	6.5	0.000704	0.002049
7	0.50817	0.69240	7	0.000630	0.002309
7.5	0.55990	0.75620	7.5	0.000651	0.002398
8	0.61630	0.81440	8	0.000653	0.002336
8.5	0.66000	0.85470	8.5	0.000691	0.002628
9	0.70190	0.88880	9	0.000698	0.002536
9.5	0.74560	0.91353	9.5	0.000713	0.002547
10	0.77793	0.93460	10	0.000657	0.002779

Table 7(a). The true-alarm rate and false-alarm rate when the standard deviation of the error term shifts from  $\sigma_e$  to  $(1+\delta)\sigma_e$ ,  $\delta=0, 0.05, 0.1, 0.15, 0.2, \dots, 1$ ,  $\sigma_e=1$ , for the case of one out-of-control profile.

True-alarm rate			False-alarm rate		
$\delta$	Bonferroni Method	Multiple FDR Method	$\delta$	Bonferroni Method	Multiple FDR Method
0			0	0.001034	0.001142
0.05	0.0031	0.0037	0.05	0.000998	0.001022
0.1	0.0117	0.0125	0.1	0.001000	0.001047
0.15	0.0359	0.0374	0.15	0.001022	0.001100
0.2	0.0919	0.0930	0.2	0.000906	0.001176
0.25	0.1796	0.1749	0.25	0.000863	0.001239
0.3	0.2934	0.3058	0.3	0.000833	0.001343
0.35	0.4325	0.4360	0.35	0.000900	0.001429
0.4	0.5850	0.5779	0.4	0.000935	0.001488
0.45	0.7035	0.7055	0.45	0.000753	0.001610
0.5	0.7937	0.8067	0.5	0.000843	0.001676
0.55	0.8645	0.8731	0.55	0.000767	0.001541
0.6	0.9193	0.9240	0.6	0.000747	0.001757
0.65	0.9506	0.9527	0.65	0.000718	0.001724
0.7	0.9746	0.9763	0.7	0.000849	0.001782
0.75	0.9840	0.9874	0.75	0.000790	0.001669
0.8	0.9909	0.9910	0.8	0.000788	0.001641
0.85	0.9959	0.9967	0.85	0.000771	0.001637
0.9	0.9978	0.9975	0.9	0.000700	0.001565
0.95	0.9990	0.9983	0.95	0.000763	0.001582
1	0.9993	0.9993	1	0.000724	0.001680

Table 7(b). The true-alarm rate and false-alarm rate when the standard deviation of the error term shifts from  $\sigma_e$  to  $(1+\delta)\sigma_e$ ,  $\delta=0, 0.05, 0.1, 0.15, 0.2, \dots, 1$ ,  $\sigma_e=1$ , for the case of two out-of-control profiles.

True-alarm rate			False-alarm rate		
$\delta$	Bonferroni Method	Multiple FDR Method	$\delta$	Bonferroni Method	Multiple FDR Method
0			0	0.001008	0.001056
0.05	0.00320	0.00330	0.05	0.000971	0.000960
0.1	0.01125	0.01060	0.1	0.000858	0.001029
0.15	0.03100	0.03445	0.15	0.000985	0.001044
0.2	0.07910	0.09085	0.2	0.000902	0.001188
0.25	0.15965	0.17325	0.25	0.000954	0.001242
0.3	0.27260	0.29825	0.3	0.000810	0.001417
0.35	0.39345	0.43370	0.35	0.000781	0.001821
0.4	0.53490	0.57855	0.4	0.000783	0.001890
0.45	0.65945	0.70135	0.45	0.000740	0.001992
0.5	0.75885	0.80515	0.5	0.000775	0.002075
0.55	0.84420	0.87180	0.55	0.000706	0.002192
0.6	0.89645	0.92225	0.6	0.000729	0.002260
0.65	0.93165	0.95045	0.65	0.000656	0.002156
0.7	0.96230	0.97205	0.7	0.000669	0.002129
0.75	0.97510	0.98410	0.75	0.000658	0.002271
0.8	0.98605	0.99110	0.8	0.000715	0.002140
0.85	0.99250	0.99450	0.85	0.000608	0.002208
0.9	0.99615	0.99730	0.9	0.000646	0.002119
0.95	0.99755	0.99870	0.95	0.000642	0.002096
1	0.99860	0.99945	1	0.000621	0.002077

Table 7(c). The true-alarm rate and false-alarm rate when the standard deviation of the error term shifts from  $\sigma_e$  to  $(1+\delta)\sigma_e$ ,  $\delta=0, 0.05, 0.1, 0.15, 0.2, \dots, 1$ ,  $\sigma_e=1$ , for the case of three out-of-control profiles.

True-alarm rate			False-alarm rate		
$\delta$	Bonferroni Method	Multiple FDR Method	$\delta$	Bonferroni Method	Multiple FDR Method
0			0	0.001034	0.001106
0.05	0.00283	0.003233	0.05	0.000989	0.001068
0.1	0.00987	0.011333	0.1	0.000983	0.000934
0.15	0.03050	0.031033	0.15	0.000881	0.001081
0.2	0.07523	0.081433	0.2	0.000857	0.001206
0.25	0.14887	0.165067	0.25	0.000757	0.001326
0.3	0.25100	0.287600	0.3	0.000781	0.001613
0.35	0.37413	0.423400	0.35	0.000777	0.002019
0.4	0.50147	0.568133	0.4	0.000702	0.002134
0.45	0.62503	0.691267	0.45	0.000679	0.002385
0.5	0.72917	0.791033	0.5	0.000698	0.002647
0.55	0.80970	0.866500	0.55	0.000649	0.002696
0.6	0.87143	0.915600	0.6	0.000674	0.002751
0.65	0.91537	0.945167	0.65	0.000672	0.002596
0.7	0.94543	0.968267	0.7	0.000702	0.002781
0.75	0.96553	0.979700	0.75	0.000623	0.002674
0.8	0.97943	0.987300	0.8	0.000638	0.002609
0.85	0.98607	0.992900	0.85	0.000581	0.002638
0.9	0.99147	0.996700	0.9	0.000609	0.002562
0.95	0.99647	0.997633	0.95	0.000651	0.002526
1	0.99787	0.998567	1	0.000621	0.002694

Table 8. Detecting power of the individual X chart in Phase I. ( $\alpha=0.05$ ,  $k=50$ )

$\delta$	0.5	1	1.5	2	2.5	3	3.5	4	4.5	5
$p$	0.002706	0.011003	0.036683	0.098428	0.2146	0.385694	0.582948	0.760974	0.886753	0.956315
$\delta$	5.5	6	6.5	7	7.5	8	8.5	9	9.5	10
$p$	0.986428	0.99663	0.999335	0.999896	0.999987	0.999999	1	1	1	1



## Figures

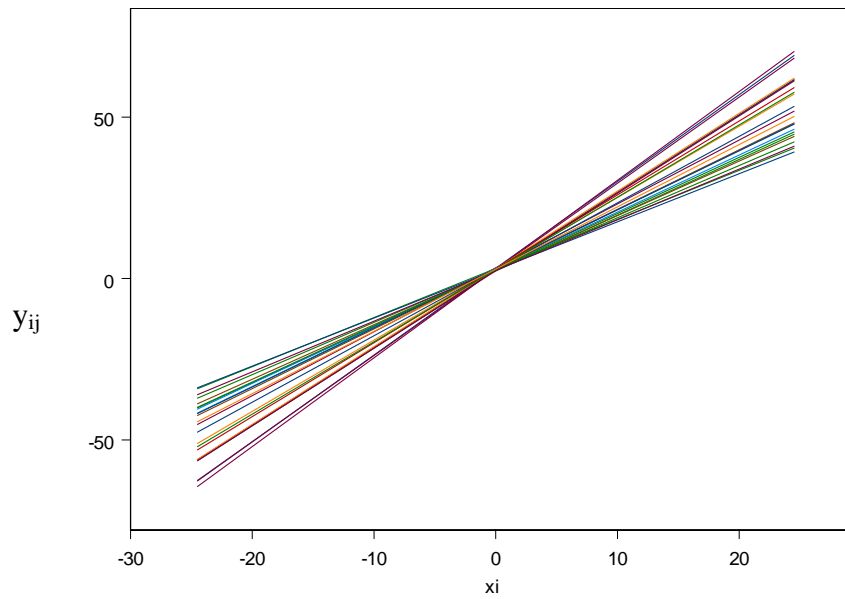


Figure 1. Twenty-five simulated profiles without error:  $y_{ij} = A_{0j} + A_{1j}x_i$ ,

where  $A_{0j} \sim N(3, 0.09)$  and  $A_{1j} \sim N(2, 0.09)$ .

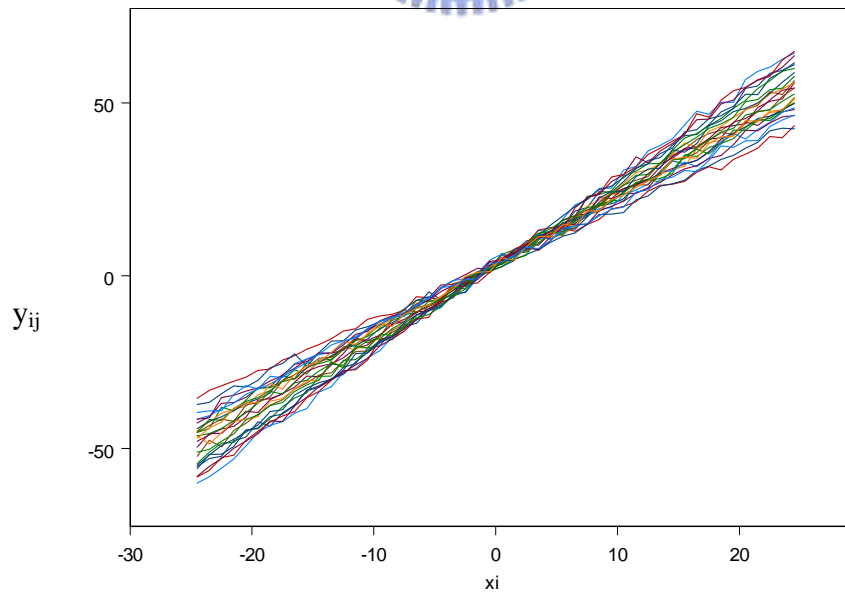
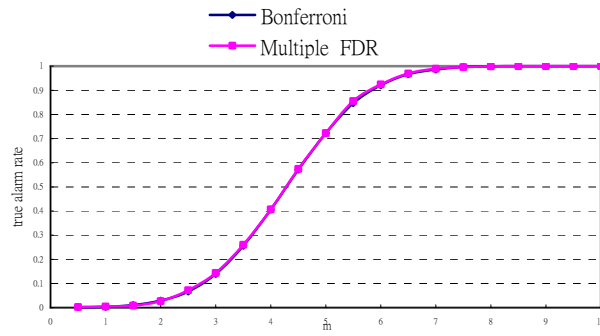


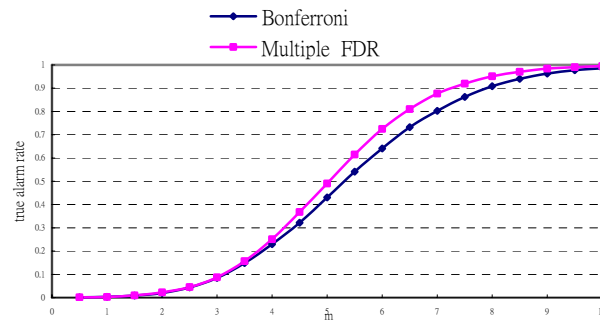
Figure 2. Twenty-five simulated profiles with error:  $y_{ij} = A_{0j} + A_{1j}x_i + \varepsilon_{ij}$ , where

$A_{0j} \sim N(3, 0.09)$ ,  $A_{1j} \sim N(2, 0.09)$ , and  $\varepsilon_{ij} \sim N(0, 1)$ .

(a) one out-of-control profile



(b) two out-of-control profiles



(c) three out-of-control profiles

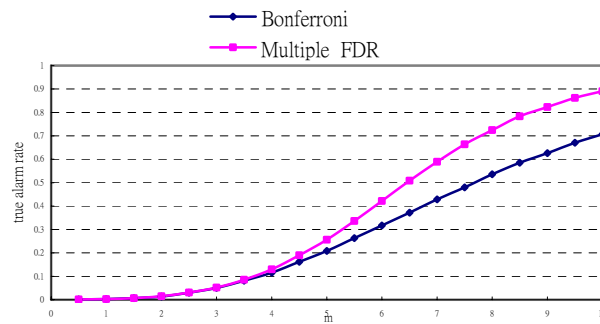
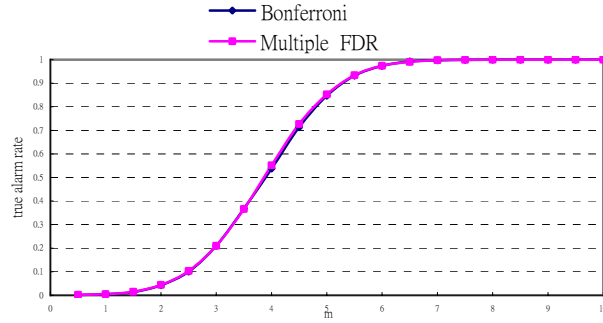


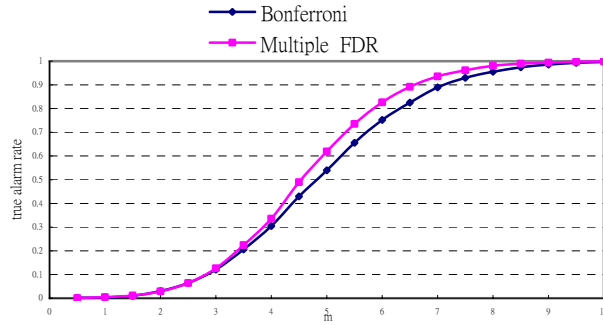
Figure 3. The true-alarm rate comparison when the mean of the intercept term shifts from  $\alpha_0$  to  $\alpha_0 + \delta\sigma_0$ ,  $\delta=0, 0.5, 1, \dots, 10$ , for the case of one, two, and three out-of-control profiles.



(a) one out-of-control profile



(b) two out-of-control profiles



(c) three out-of-control profiles

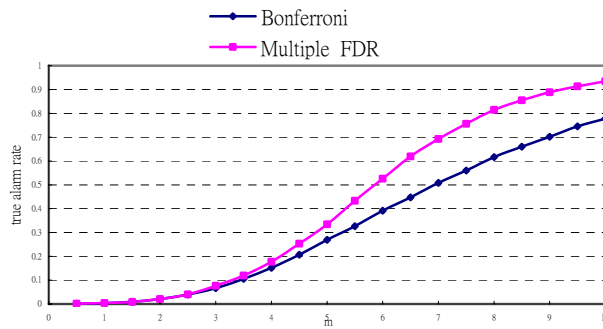
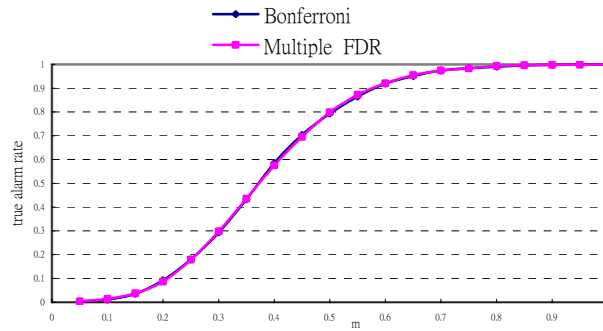
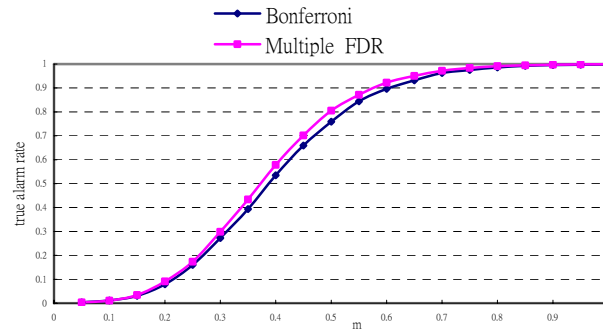


Figure 4. The true-alarm rate comparison when the mean of the slope term shifts from  $\alpha_1$  to  $\alpha_1 + \delta\sigma_1$ ,  $\delta=0, 0.5, 1, \dots, 10$ , for the case of one, two, and three out-of-control profiles.

(a) one out-of-control profile



(b) two out-of-control profiles



(c) three out-of-control profiles

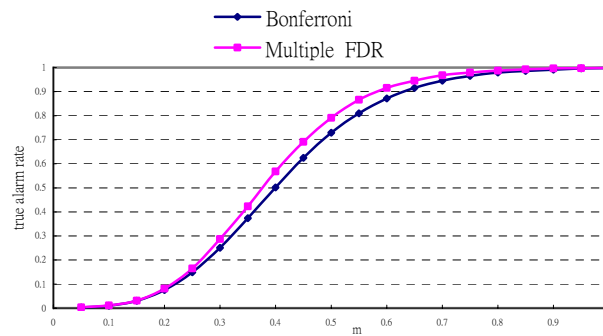
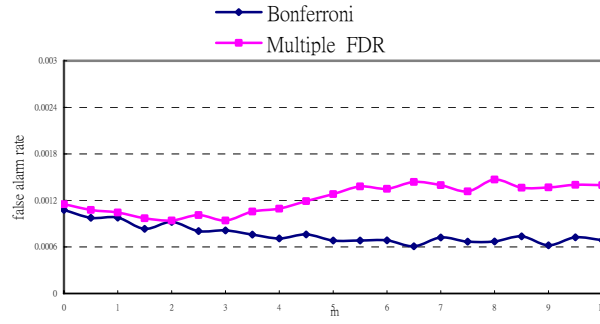
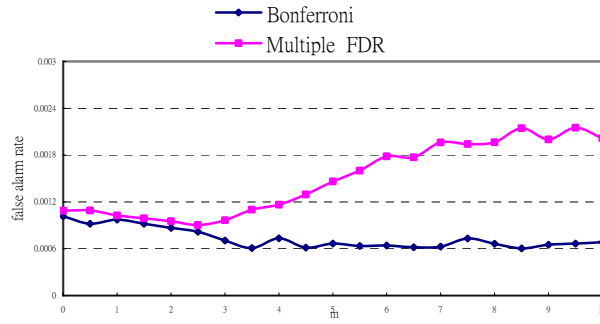


Figure 5. The true-alarm rate comparison when the standard deviation of the error term shifts from  $\sigma_e$  to  $(1+\delta)\sigma_e$ ,  $\delta=0, 0.05, 0.1, 0.15, 0.2, \dots, 1$ , for the case of one, two, and three out-of-control profiles.

(a) one out-of-control profile



(b) two out-of-control profiles



(c) three out-of-control profiles

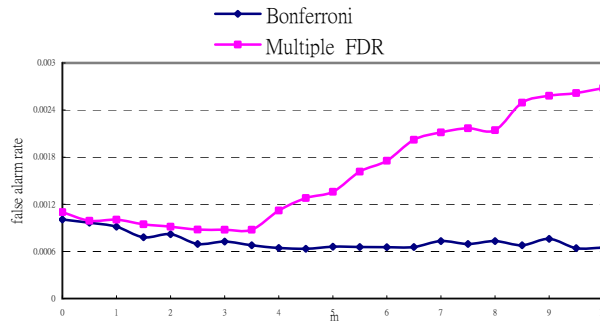
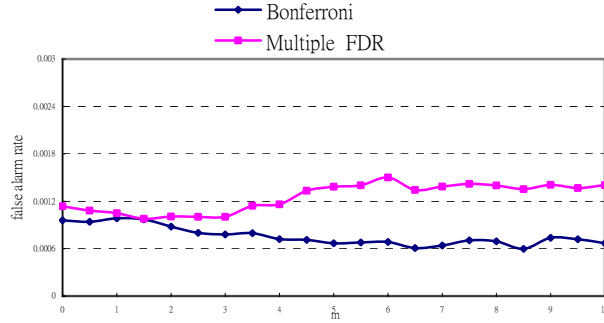
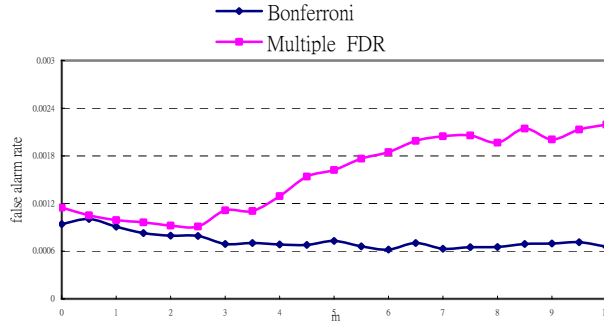


Figure 6. The false-alarm rate comparison when the mean of the intercept term shifts from  $\alpha_0$  to  $\alpha_0 + \delta\sigma_0$ ,  $\delta=0, 0.5, 1, \dots, 10$ , for the case of one, two, and three out-of-control profiles.

(a) one out-of-control profile



(b) two out-of-control profiles



(c) three out-of-control profiles

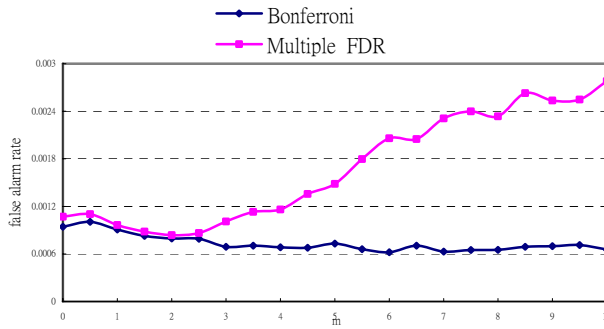
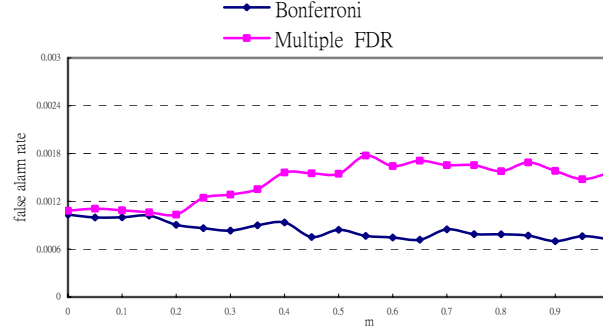
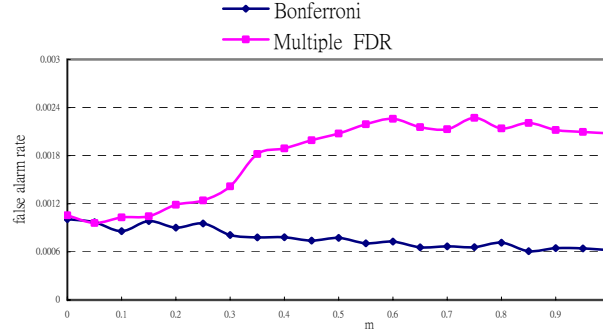


Figure 7. The false-alarm rate comparison when the mean of the slope term shifts from  $\alpha_1$  to  $\alpha_1 + \delta\sigma_1$ ,  $\delta=0, 0.5, 1, \dots, 10$ , for the case of one, two, and three out-of-control profiles.

(a) one out-of-control profile



(b) two out-of-control profiles



(c) three out-of-control profiles

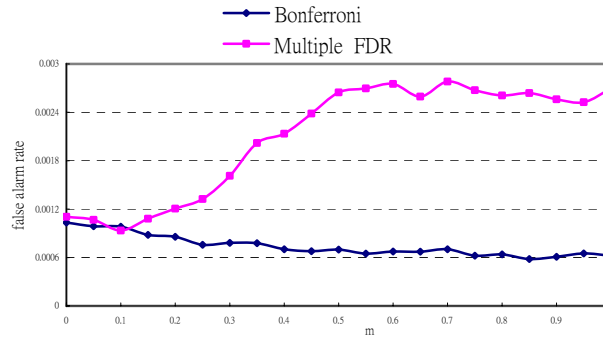


Figure 8. The false-alarm rate comparison when the standard deviation of the error term shifts from  $\sigma_e$  to  $(1+\delta)\sigma_e$ ,  $\delta=0, 0.05, 0.1, 0.15, 0.2, \dots, 1$ , for the case of one, two, and three out-of-control profiles.